DETECTION OF INCIPIENT SLIP IN CHILD-SIZED MYOELECTRIC HANDS

by

Shechar Dworski

A thesis submitted in conformity with the requirements for the degree of
Master of Science
Institute of Medical Science
Institute of Biomaterials and Biomedical Engineering
University of Toronto

ABSTRACT

This thesis is a continuation of research and development done at Bloorview MacMillan Centre in the area of slip detection for children's myoelectric hands. This project took the research into a new and more practical direction, bringing the concept closer to clinical implementation. Initial work in this project was based on addressing concerns and recommendations laid forth by previous researchers in the field. The first issue that was addressed was the motor that powered the hand. Previous work used a large, low-geared motor. This research tested the characteristics of the original, small, highly geared motor used in a clinical prosthetic hand, and allowed the slip detection system to work with this motor. The next issue looked at was the use of compliant fingertips with the slip detection system. The use of piezoelectric polymer (PVDF) slip sensors allowed for compatibility with compliant fingertips, whereas earlier research used incompatible piezoelectric ceramics (PZT). These new sensors also allowed for the slip detection system to work in the presence of a cosmetic PVC glove, which was previously a clinically limiting problem. Analogue signal processing circuitry was built to allow for electronic miniaturization for housing within the prosthetic hand. The circuit was designed to minimize noise from electromagnetic interference and from external non-slip mechanical vibrations. The effect of sensor placement and positioning was tested for optimal noise cancellation. The complete slip detection system was built and tested with a real-life slip situation, and was shown to react to slip satisfactorily. While much of the noise from external vibration was reduced, some response was seen to this noise under certain test conditions. Other test conditions showed little or no response to noise. The system's response to slip was better with the cosmetic glove on.

ACKNOWLEDGMENTS

I would like to thank my supervisors, Dr. Naumann and Dr. Milner for giving me the opportunity to do this work , and for the privilege of working with them. They provided me with great support, encouragement, and advice at all times. Without their help, this thesis would not have been possible.

Thanks to all the staff, researchers, and technicians at Bloorview MacMillan Centre, whose friendly and helpful attitude guided me through this project and helped me through some of the rough spots along the path. The insight and resources they provided went a long way in directing my research.

Thanks to the other graduate students at Bloorview MacMillan Centre and at the Institute of Biomaterials and Biomedical Engineering for all their input and suggestions. They helped make my stay more enjoyable and memorable.

Thanks most of all to my family and friends, who were there for me throughout this project, and have been there with me all along.

Funding for this research was provided by the Natural Sciences and Engineering Research Council of Canada.

ABBREVIATIONS

AC	Alternating Current
BMC	Bloorview MacMillan Centre
DC	Direct Current
EM	Electromagnetic
FSR	Force Sensitive Resistor
IC	Integrated Circuit
IA	Instrumentation Amplifier
MSI	Measurement Specialties Incorporated
NR	Noise Reduction
PVC	Polyvinyl chloride
PVDF	Polyvinylidene Fluoride
PZT	Lead Zirconate Titanate
SNR	Signal to Noise Ratio
VASI	Variety Ability Systems Incorporated

TABLE OF CONTENTS

LIST OF FIGURES

LIST OF TABLES

LIST OF EQUATIONS

Page

1. THESIS OVERVIEW

1.1. INTRODUCTION

A prosthesis is a man-made device meant to replace a natural body part that is either not functioning properly or absent. The main purpose of the prosthesis is to emulate the part of the body that it is replacing as closely as possible. It should perform the same functions, or better, with minimal liabilities or side effects to the user. In the design of prostheses, a close understanding of the natural system and its environment is needed. This is to ensure that the prosthesis performs the same functions as the natural system. At first the design should focus on the major, basic functions of the system it is replacing, and then evolve to include finer aspects, in an effort to come closer to truly mimicking the original system. At the same time, care must be given to ensure that the prosthesis does not significantly interfere with other systems and functions in its environment. Prostheses exist today for almost any body part. Perhaps one of the oldest types of prostheses is the artificial limb. Since external prostheses do not interfere with the body's internal mechanisms, the design of artificial limbs began long before understanding of the inner functions of the human body began. The earliest artificial limbs could be found even in the imagination of a child daydreaming of pirates, as a simple hook for a hand, and a wooden column for a leg. While not mimicking the human hand and leg exactly, even these crude devices performed the most basic tasks: a way in which to grasp certain

objects, and a support on which to walk. However, not all objects could be grasped with a hook, and not all terrains could be easily or comfortably traversed with a wooden leg. So the endeavor began to improve the function and cosmesis of artificial limbs, a process which attempts to converge at complete emulation of a human limb: an artificial limb that can do all that a human limb can.

Perhaps the portrayal of artificial hands in popular culture has led to the belief that an artificial hand may one day not only perfectly replace a natural limb, but also out-perform it. While this may be possible, the state of the art today is not quite that advanced. The quest to understand the human body is still continuing, and research and development in prosthetics is coming closer to replicating the human body. This thesis specifically focuses on the feature of tactile sensing. However, this type of tactile sensing is not of the variety that the user can consciously feel, but one that is part of an automatic slip detection system, very much like a reflex in the natural hand. This system has touch sensors on the finger that can tell if an object being held is beginning to move, or slip. Upon detection, this system then automatically increases the grip force until the object is once again held securely. This system is useful on its own, but when used as part of a greater system, it can allow the hand to detect the optimal grip force for any given object. This property would allow light, fragile objects like an egg or a plastic cup to be gripped with the same ease as heavy objects requiring greater grip force, since the system automatically selects the most appropriate grip force; the minimum force required such that slip does not occur.

1.2. OBJECTIVE

The purpose of this project was to bring the slip detection system closer to clinical implementation by addressing the critical problems outlined in previous work in the field. These problems, which are outlined in Section 1.5, had put limitations on the clinical implementation of the slip detection system. The goal of this project was to provide simple, inexpensive, and practical solutions to these problems so that the system could begin to undergo clinical testing. Part of this goal was to analyze and characterize the slip detection system, so as to bring new insights into solving the problems previously associated with it.

1.3 HYPOTHESIS

The prosthetic hand acts as a mechanical system. Slip vibrations and noise vibrations propagate through the hand based on the properties of this mechanical system. It is hypothesized that the problems raised in previous work (such as discriminating noise vibrations from slip vibrations) can be solved by exploiting the system properties. This could be done by controlling sensor placement and positioning, using compliant fingertips, and modifying the sensor output with an appropriate electrical system that interfaces with the hand controller. The overall result would be an automatic closing response to slip, just like the one seen in the natural human hand.

1.4. SIGNIFICANCE

Slip detection is a property of myoelectric hands that has been thought to be desirable by prosthetic researchers and clinicians. Such a system would allow the user more freedom from conscious manipulation of objects and increased ease of grasping objects and holding on to them without dropping them. As part of a grasping algorithm system, slip detection would allow for finer grasping control, and easier use. An automated means for finer grasping would be especially beneficial for people with bilateral amputations, who rely on their prosthetic hands for all their grasping. The benefits of automated grasping control would be especially relevant to children, who have less grasping experience than adults, and, as such, would stand to benefit the most from an automatic grasping and slip detection system.

1.5. OVERVIEW OF THESIS

The work of this thesis continued from the previous work [1, 2, 3, 4] by looking at the recommendations made for future work and trying to address the issues raised. This, in turn, led to new issues and ideas, which were dealt with as the work progressed.
The relevant issues that were considered at the beginning of the project, in order of importance in which they needed to be addressed before further work could be done, were:

1. The motor: The properties of the VASI 5-9 motor and gear system needed to be characterized first, so they be could be used in the final design. In previous work at BMC [1], the original VASI 5-9 motor and gearing were replaced with a larger motor with a lower gear-ratio to simplify the design and testing.
2. Compliant fingertips: A design for the sensors and their attachment to the fingers had to be created as to allow them to be compatible with compliant fingertips.
3. Miniaturization: The control circuitry had to be designed using hard-wired electronics that would fit within the VASI 5-9 hand. Previous work at BMC [1,2] used a desktop personal computer and ran software to implement the control scheme.
4. Noise cancellation: The noise cancellation algorithm and strategy had to be worked out to maximize the signal-to-noise ratio of the sensors and to minimize noise from external banging. This proved to be the major and most involved part of the work. Sensor placement had to be considered, and the signal processing circuitry had to be designed, evaluated, and redesigned repeatedly until satisfactory results were achieved.
5. Cosmetic glove: The sensors' placement and design, together with the signal processing circuitry had to be considered in the presence of the cosmetic PVC glove, so that the glove would not impede the proper functioning of the system.
6. Prototyping and testing: The completed design had to be tested to make sure that it worked as a whole in its intended application, once all the parts were seen to work on their own under laboratory test conditions.
7. Clinical testing: The completed, working prototype needed to be tested under clinical

conditions to evaluate the effectiveness of slip detection. This would involve having children who normally use a prosthetic hand trying the new hand design, and evaluating whether slip detection confers any significant advantage. This stage was not reached in this project.

1.6. OVERVIEW OF CHAPTERS

There are six main chapters and seven appendices:

- Chapter one gives a brief introduction and overview to the project.
- Chapter two provides relevant background information on different topics relating to prosthetic hands, and ends with a description of some other current research projects relevant to myoelectric hands, such as compliant fingertips and sensory feedback.
- Chapter three goes into detail about slip detection. It outlines previous work done on slip detection at Bloorview Macmillan Centre, from which this project stemmed, as well as other research in the field.
- Chapter four describes the experimental design and approach taken, detailing the materials and equipment used and their purpose in the design process, as well as some of the basic ideas behind the design.
- Chapter five outlines all the individual experiments performed with each design, and discusses how the results from one test design led to the next experimental design. The results are presented and interpreted in the logical chronological order in which the design evolved.

- Chapter six summarizes and concludes the thesis with recommendations for future work.
- Appendix A includes background information on systems theory and mathematics needed to understand the thesis, as well as a description of the physiological slip detection system. It is intended for readers who have a background in biology, but lack the understanding of basic engineering principles.
- Appendices B-E contain electronic parts specifications.
- Appendices F-G contain diagrams of the circuits used in this thesis

2. BACKGROUND

2.1. HISTORY OF PROSTHETIC HANDS

2.1.1. Prosthetic Hands

While the human hand may not be necessary for the basic life functions in the same way that the heart or lungs are, its functions are numerous, and are also culturally and socially significant. The hand and its basic functions may seem simple at first glance, but closer inspection shows the hand to be a highly intricate device, with a built-in capacity for countless functions. Some of these can be seen in the playing of musical instruments, typing, self-defense, manipulating objects, and a variety of other learned activities. Anthropologists have even speculated that it is the versatility of the human hand that led to the creation of civilization. The hand functions largely on a subconscious level, and, as such, the user may be unaware of the intrinsic complexities involved in performing even the simplest of tasks. These complexities become apparent when one attempts to design an artificial hand.

In the past, the most basic hands had no moving parts. A wooden, metal, or wooden/metal hybrid device was attached to the stump. At the end of the prosthesis, a hook, or other grasping implement was attached that could perform very limited functions, such as holding an object in place[16]. In more advanced hands, the end-effector could be switched depending on the task, such as a fork or spoon for eating. The next class of artificial hands involved moving parts. A moving part could include any major

joint or hand motion, such as opening and closing a hand in a set finger position, wrist rotation, elbow movement, and shoulder movement. These hands were body powered. This meant that the moving part of the hand was connected via mechanical conveyers, such as cables, to other parts of the body which were capable of creating movement. For example, a moving artificial elbow might have cables connected to it that led to the opposite shoulder, and, by moving that shoulder forward and backward, the cables pulled on the elbow and effectively caused it to bend and extend. In this way, the power needed for movement in the prosthesis came from the user's body. Since the human body can produce substantial forces, this method was effective, and is still used today by many prosthesis wearers, who choose it over the more recently available electrically powered prostheses [17]. The advent of electronics allowed batteries to provide the power for joint movement. Pistons, hydraulics, but usually electric motors were used to power the movement of a hand part, and the signal to activate the motor came from a mechanical switch located where the user could easily access it. The only effort needed was that needed to operate a switch, which requires much less energy then using a body powered hand. The reasons people today still choose body power over electrical power are independence from an external power supply which needs constant recharging, a more reliable mechanism, and decreased weight [16]. Also, the user has an increased sense of connection with the prosthesis when it is body-powered, and feels more involved with its activities, since the motions and power come directly from their body. There is also a greater sense of feedback, as the user can feel how hard they are pulling or pushing to make the hand move. Also, some vibrations created at the hand when it touches object or bangs are transmitted along the cables and may be detected by adept users.

2.1.2. Myoelectric Hands

The next stage in development, and the current state of the art in commercially available prosthetic hands, are hands that are myoelectrically controlled. Before myoelectric control, electrically powered hands had to be controlled using an external switch, such as a conveniently situated button key-pad or a lever switch. In myoelectric control, the user contracts their muscles to send a signal to an electrically powered hand. Whenever a muscle contracts, it produces measurable electrical activity, so much so that it is detectable on the skin surface. Special myoelectric sensors are very sensitive, and when placed on the skin above an active muscle, they can accurately detect when and how much it is contracted, by sensing the changes in electrical activity. This muscle signal is called an electromyographic (EMG) signal. The EMG signal is amplified, rectified, filtered and sent to a circuit that controls the motor of a prosthetic hand, which then opens or closes a hand's end effector, rotates a wrist, or flexes and extends an elbow. Currently, only two sensors are used, and they are placed over antagonistic muscle sites, such as the upper arm biceps and triceps, or the forearm flexors and extensors [15]. In this way, the two opposing muscles produce two opposite results in the prosthesis. For example, a control scheme could be set up so that contracting the biceps causes the hand to close and contracting the triceps causes the hand to open. A prosthetic wearer can usually learn how to use this system quite rapidly.

Many users become very adept at using a two site control scheme, and are able to turn the hand into a versatile instrument [29]. While these users can perform many more functions than with a simple, non-moving hook, they are still far from being able to emulate the

functions of the natural human hand. They can only move one joint in two directions (two degrees of freedom), and have no sensory feedback from the hand. Current research in prosthetic hands attempts to emulate the natural human hand by providing sensory feedback to the user and allowing more functions (greater degrees of freedom) by improving hand design, and finding new control methods.

Another point that should be mentioned is cosmesis. An artificial hand should look very much like a natural human hand. Part of artificial hand research and development is finding new designs to make the outer layer of the hand, not just the inner workings, seem more realistic. Today, a PVC glove, molded and colored to look like skin is used to cover the hand to make it look real [15]. This is important for social and psychological reasons, as a person is more likely to feel like they fit in with society and will be more likely to use the hand if it looks natural.

2.2. CHILDREN WITH AMPUTATIONS

Most amputations in children are congenital; that is, the amputations are present at birth as a result of incomplete development. In adults, most amputations are traumatic, as a result of an accident or disease [4]. The significance of this is that most children have no memory or learned skill when it comes to their amputation, and therefore, it seems reasonable that they may take longer to master grasping techniques with an artificial hand. On the other hand, they are not habituated by previously learned patterns and may be more adept at using the prosthesis with practice. Most amputations of the arm are

unilateral, that is, one hand only. Children use their natural hand to perform fine grasping tasks, and the prosthetic hand for support only when needed. Bilateral amputations comprise 15% of people with upper extremity amputations, who are much more reliant on their prostheses because they use them for all their grasping needs [4]. For them, an artificial hand capable of fine grasping is critical for being able to perform more delicate tasks. Since they use their artificial hands the most, they are likely to benefit the most from any advancements.

2.3. VASI AND BLOORVIEW MACMILLAN REHABILITATION CENTRE

Variety Ability Systems Incorporated, or VASI, is a major producer of prosthetic hands and other rehabilitation devices for children. Originally started as The Variety Village Electrolimb Production Centre in 1970, its main focus has been on meeting the needs of children with disabilities [21]. Bloorview MacMillan Centre (BMC) is a rehabilitation hospital and research centre in Toronto that works closely with VASI and services greater Toronto and clients from across Ontario. Its focus is on children and young adults with disabilities, and its services range from assistive seating devices to fitting prosthetic hands [22]. It also houses a research program that aims to advance and develop products in all areas of rehabilitation. The program is operated by BMC and VASI employees, along with graduate students from the University of Toronto. The research presented in this thesis, along with other current and recent advancements presented, was carried out at BMC.

2.4. VASI HAND FEATURES

The current VASI hand comes in the following sizes, depending on the child's age: 0-3, 2-6, 5-9, and 7-11 years of age.

Figure 2.1. VASI hands from left to right: 0-3, 2-6, 5-9, 7-11. [23]

The hand has a soft glove to cover it, for protecting the inner mechanisms, and to give it a skin-like colour and appearance.

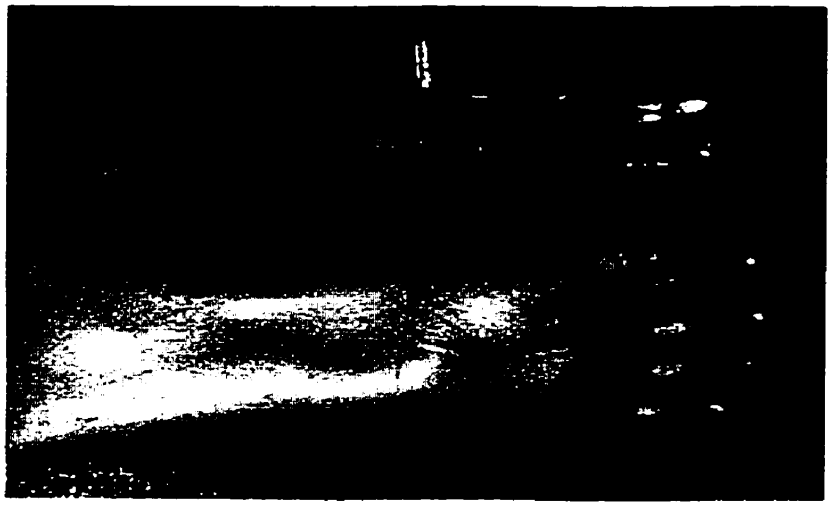

Figure 2.2. VASI 5-9 Hand next to PVC glove covering.

The glove comes in many colours, to match the user's natural skin colour. The hand uses one rechargeable six volt battery that lasts for the duration of one day and is recharged at night. The standard myoelectric controller has some useful features. An energy saver unit turns power off to the motor when it is being powered but has reached its limit of motion. A proportional force controller allows the hand to be closed and opened at different speeds, depending on the magnitude of the myoelectric signal. In other words, the harder and faster a muscle is contracted, the faster the motor acts to close or open the hand. A relatively new feature is called MyoMicro. It uses a small microcomputer to allow the user to program different control schemes in the hand. The schemes are programmed through a desktop computer program and then recorded in the controller's memory [27]. The main purpose of this controller is to allow the rapid customization of a control strategy for an individual. While, in theory, almost any control pattern can be programmed, the most common ones are as follows. An open and close signal opens and closes the hand respectively. If both the open and close signals are applied at the same time, the control switches over to the wrist. Then, one signal turns the wrist clockwise, and the other signal turns it counterclockwise. An elbow joint could also be added to this routine. Another scheme depends on the speed or intensity at which the muscle is contracted. A quick contraction in one muscle might open the hand, while a slow contraction closes it. At the same time, a quick contraction of the other muscle turns the wrist one way, while a slow contraction of that muscle turns it the other way [27]. The reason this controller scheme is useful is because current technology can only separate between two types of antagonistic muscle contraction patterns in a given area. That level of control is termed two degrees of freedom. This controller can take a two degree-of-

freedom system and turn it into a multiple degree-of-freedom system.

2.5. RECENT RESEARCH AT BMC

2.5.1. Myoelectric Pattern Recognition

Another way to add degrees of freedom to the artificial hand was the subject of a recent research project at BMC. Kennedy (1998) [19] investigated the possibility of distinguishing more than two muscle patterns at the forearm sites of people with below-elbow amputations. In this control scheme, the user would use up to six different motions to control the hand, and each one would signal a different function. These muscle patterns correspond to the muscle groups that would be used to move a hand up and down, side to side, and rotate the forearm in both directions. While it was found that it is easy to consistently distinguish between the up and down muscle patterns that are use to control current prostheses, other muscle patterns were not as distinguishable. It was thought that with some training, however, the user could learn to create more distinct patterns and thereby signal a multiple degree of freedom artificial hand. Additional degrees of freedom could be wrist rotation, elbow movement, or individual finger movement.

2.5.2. Adaptive Grasp Hand

Another project at BMC, by Dechev (1998) [20], attempted to emulate the movement of a hand in which every finger moved individually, but with only a two degrees of freedom controller. This was called an adaptive grasp hand, because as it closed around an irregularly shaped object, the fingers curled around the object, as if each finger moved on

its own. The hand was designed such that when one finger met resistance, it would stop but the other fingers would continue to close. The overall effect was a grasp that conformed to the shape of an object, and therefore held it better. The hand and the grasp also looked very natural, more similar to a true human hand than other currently used prosthetic hands. The overall grip force achieved, however, was an order lower than that of current hands.

2.5.3. Compliant Fingertips

Another feature that has been investigated at BMC is compliant fingertips [3]. With this feature, the fingertips, or even the entire front parts of each finger, are made of a soft rubbery material, more similar in consistency to human flesh. Currently, VASI hands are made of a tough plastic, with a soft glove covering. While the glove provides some absorbency of force, it is relatively thin, so that even with the glove on, the fingertips do not conform to an object's surface geometry. Compliant fingertips are advantageous because they provide a sturdier grip of objects, and allow smaller objects, as well as irregularly shaped or smooth slippery objects to be grasped more effectively. The reason for this is that as a compliant finger presses down on an object, the finger surface expands and surrounds the object surface creating a larger contact surface area. If the finger were rigid, it would only touch the object on the smaller surface where it touched. The compliant finger conforms to the object's surface geometry, increasing the contact surface area, which makes it easier to grip the object. Picking up a plastic pen on a table would be hard with a rigid fingertip, since there is not much contact area between the fingertip and the pen. A compliant fingertip creates a pad in which the pen is held firmly.

Also, objects held within compliant fingertips are more stable within the grip, because the increased contact area creates an increased frictional force, which makes it harder for the object to become dislodged. The contact area also becomes more elastic, so that an initial disturbance force goes into creating an elastic deformation in the fingertip. Only when additional force is added, beyond the force absorbed by elastic deformation and static friction, does a disturbance force act to cause movement in the object.

Joiner [3] researched the best kind of material to use for the compliant fingertip. Silicone was found to be the best material. He also tried to determine the best place to put the compliant material on the finger, and found that inlaying the entire finger front, not just the tip, was most useful. He also found that adding a small overlaying ridge on the fingertip, similar to where a fingernail would be, increases grasping ability. This little ridge helps to pick up small and slippery objects, like a pen or a paperclip, much in the same way that a natural fingernail does.

2.6. SENSORY FEEDBACK

Many features of artificial hands focus on increasing the user's ability to operate their prosthesis. An artificial hand should give the user some sensory feedback, if it is to behave like a natural human hand. The most basic feedback available to the user is visual. The user sees the hand moving, its position in space relative to the body and to objects, and its effect on objects. If a grip is too tight, deformation of an object may be seen. If it is too loose, the object may be seen to fall. It would be more convenient if the

user could feel the hand, and sense what it is doing directly without relying on visual cues. One type of direct feedback that is being researched at other research centres is pressure feedback. This feature allows the user to feel how strong the pressure at the fingertips is; that is, how hard an object is being gripped. This works by using pressure sensors on the finger to detect the amount of force pressing down on the finger. This signal is processed and sent to a device connected to the user at the remnant limb. The device could be a pressure cuff that squeezes harder with increased pressure at the finger[10]; a vibration, or a mild electrical tingling, which increases in magnitude as the force applied to the finger increases [9]. Some concerns with this type of feedback are that the user will become accustomed to the sensation and stops noticing it after a while, and that tissue irritation may occur in the long term [11]. Another possible type of feedback is temperature. At the Sabolich Research and Development Center in Oklahoma City, prototypes for both temperature and pressure sensory feedback systems are being tested. Temperature sensors on the finger convey this information to the user through a variable temperature plate connected to their remnant limb[12]. Research is still continuing in the hope of bringing these features into dependable, commercially available hands.

2.7. GRASPING ALGORITHM

When grasping an object, the user can only guess as to how strong a grip is required, that is, when to stop signaling to close the grip. The user relies on visual clues [4], on previous knowledge about the object, and on previous experience with the object, if any. These clues may be quite limited for young or new users. Unilateral (one side only) amputees

use the prosthesis mainly as a support for the dominant natural hand, while bilateral (both sides) amputees need to use the prosthesis for all their manual tasks. Thus, the limitations of current prostheses are especially seen for bilateral needs, since no natural hand is available for fine and precision grasping. It is in these cases that increased grip sensitivity is needed the most.

When the user cannot tell how strong their grip is, it results in several problems. Holding brittle objects becomes risky, as damage can be easily caused. Holding heavy or slippery objects involves trial and error, since the object will keep slipping until a sufficient force is reached. However, applying the maximum force initially may result in damaging the object, so the sufficient force required has to be learned or guessed, which may be challenging for young users. If this force is surpassed, in some cases by only a small amount, an object may become damaged. As well, once an object is being held, an attempt to use it as a tool may result in the object's dislodgment from the grip. The only way the user can compensate for these effects is to observe the object for signs, such as deformation in case the grip is too strong, and constantly check the position of the object in the grip to make sure it's not moving. In addition, some hand designs, particularly the VASI hand used in this project, obscure the user's view of the grasping area, making visual feedback more difficult. Since there is presently no other feedback method available to the user, the lack of visual feedback increases the difficulty and skill required in grasping objects [4]. To remedy this situation, a new design is proposed, which uses the slip system as part of a grasping algorithm. This design involves the use of pressure sensors on the fingers. These are not for giving direct sensory feedback to the user

necessarily, but for use with an automated grasping algorithm. Of course, if a viable method of providing sensory feedback becomes available, this signal could also be used for that purpose, in addition to its use in the grasping algorithm.

A pressure sensitive component would be attached to the finger surface, under the compliant fingertip. The specific component would depend on availability, but would most likely be a force sensitive resistor, as these are the most common, simple, and inexpensive pressure sensors available today. The signal from this sensor would go to the control circuitry. There would be sensors on both the thumb and the forefinger. These would allow the control circuitry to know when the thumb or finger is touching an object. If the technology became available, the user would also know this through a tactile feedback element, most likely a mechanically vibrating element in contact with the user at a site close to the amputation. Pressure at the sensors would cause a proportional vibration at the tactile element, which the user would be able to feel. The sensations for the thumb and fingers would be different as a result of using different frequencies for each signal. In this way, the user would be able to tell if the thumb, finger, or both are in contact with an object. The pressure signal would be proportional, although the proportionality would only serve to give the user a sense of varying grip pressure. As far as the control circuitry goes, it only needs to know if the signal is on or off, that is, above or below a low threshold, set at the value of pressure of just barely touching an object. The control algorithm is outlined in Figure 2.3. In the figure, P1 and P2 are the pressure sensors, and P=1 indicates above threshold activity. The user selects an object to be grasped, and then attempts to make contact with it using either the thumb or the forefinger. If the grasp is successful and in the right region of the finger, the user would

feel this as a tactile response in the form of a unique vibration. This would reduce the need for visual feedback to see if the hand is in the right position for grasping. Then the user would myoelectrically instruct the hand to close. When the hand is closed around the object, that is, when the complementary digits make contact with the object, a second unique tactile signal is felt by the user concurrently. The combination of both signals indicate to the user that the grasp is complete and the object may be moved or lifted. Otherwise, if no sensory feedback is available, the user can decide visually if the object is in position and ready to be picked up with the prosthesis. At this point, the hand would be gripping the object with a minimum preset contact force, since the motor is turned off when both contact signals are present. The control system would then switch to slip detection mode. If the grip force is insufficient, the object would start to slip as soon as it starts to be lifted and the hand would automatically increase the grip force until the slip stops. The user can overrule the slip system by giving a close signal for more than two seconds, in case full grip force is desired, such as for squeezing toothpaste out of a tube. (See Figure 2.3 on the next page)

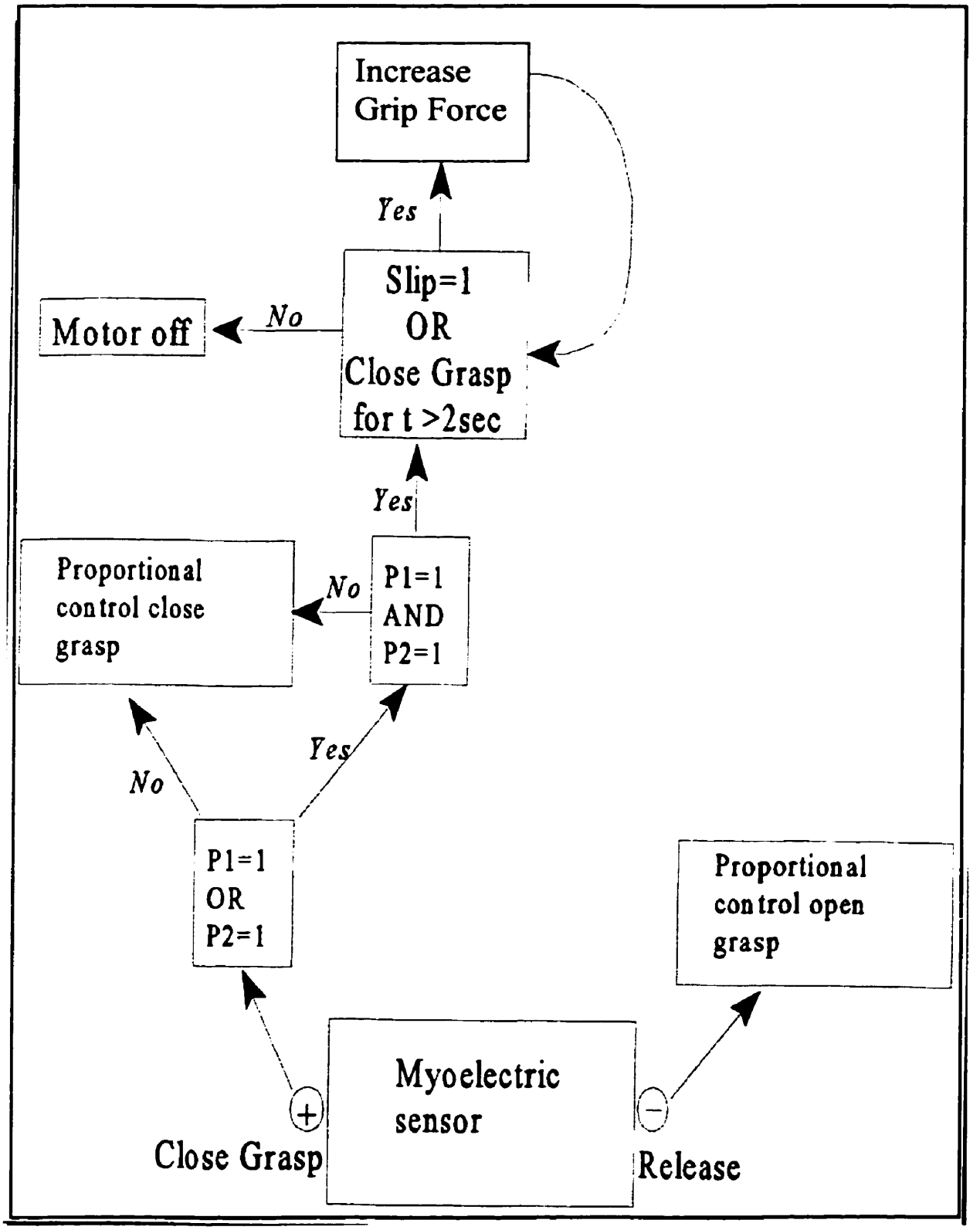

Figure 2.3. Grasping Algorithm

Another way to look at this is as a two-state system. One state of the system is activated when both the pressure sensors are in the "on" state, that is, when both sides of the grasp are experiencing pressure. In this case, the system switches to slip detection operation, and the only direct control the user has is in opening the grasp. The other state is switched on when the conditions for the previous state are not met, that is, only when one or none of the sensors are receiving input. In this case, the user has direct proportional control over the prosthetic hand and can open and close the hand as desired.

The overall effect is that each object is held only with the minimum amount of grip force necessary to allow for a stable grip. This means that light, fragile objects, as well as heavy, slippery objects, can be handled with equal facility, since the system will automatically produce the appropriate grip force. There is a maximum grip force, determined by the mechanical design of the hand, above which slip cannot be prevented. The maximum and minimum forces are properties of the hand. Each object will have three regions corresponding to three ranges of normal force. The object will slip from grasp in the region between zero and a certain value of force determined by object weight, surface geometry and surface friction. In the next range up, the object will be held securely. After a certain value of normal force, the object will break under the pressure. This point may be higher for harder objects. For brittle objects, the middle stable region is very small, and is hard to reach using trial and error. The control algorithm allows this region to be approached from below, and once it is reached, the normal force is fixed, so that the breaking point is not reached. Figure 2.4 illustrates this.

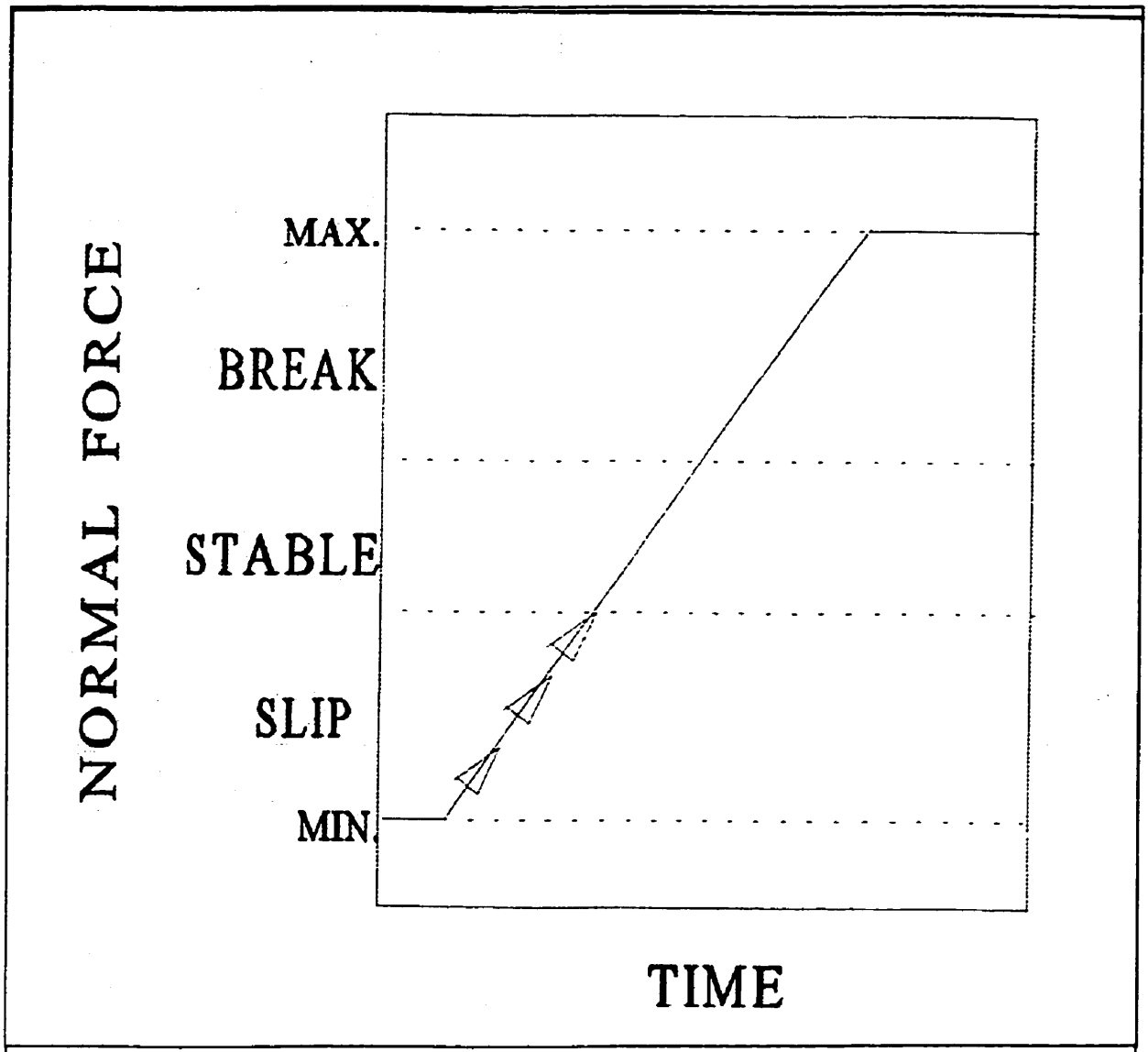

Figure 2.4. Grip Force Regions

Since the maximum and minimum forces available are independent of the three regions, the alignments may vary with different objects. The example in Figure 2.4 shows a stable region that is within the range of force that the hand can produce. The maximum may be below the stable region, in which case no stable grip is possible. The maximum may be below the break point, but above the stable point, in which case breaking is

avoided completely. In other cases, the stable region may be so large that the entire range of the hand grip-force lies within it. In any case, the minimum normal force is the starting point of the grip force in this control scheme, and the beginning of the stable region is the end point. Large disturbances may cause the grip force to increase, which is fine as long as it remains below the break point. This result is likely, since a disturbance large enough to cause such a big reaction would likely dislodge the object before the hand can react. This is unavoidable, and even the natural human hand can not react fast enough to a sufficiently large disturbance.

3. SLIP DETECTION

3.1. INTRODUCTION

A feature that incorporates both sensory feedback and improved grasping performance is slip detection. Slip occurs when an object being held begins to physically move within the grasp, due to an external force. This force could be gravity, a banging of the hand, or an attempt to use the object as a tool, such as using a knife or a pen, in which the held object is pressed against another object, subjecting it to increased forces. If slip occurs for a long enough time, the object becomes dislodged from the grasp. The aim of slip detection is to notice when slip begins, even before it is visually noticeable, and increase the grip force sufficiently until it stops. This prevents the object from becoming dislodged or significantly displaced within the grasp, without the user consciously paying attention to this matter. As such, the user could focus on object manipulation without having to think about maintaining the proper grip force, as the slip detection feature would do this automatically.

Sensors on the fingers that pick up vibrations detect slip. Vibrations are created whenever an object slips. The vibration results from the friction between two objects. As an object slips on a surface, the friction between them causes the object to stick sometimes, and then slide free, on a microscopic level [5]. When this happens, it results in

a vibratory movement, which can be detected by fine instrumentation, such as the kind used in this project. This can be observed audibly by rubbing any two surfaces together, very close to the ear. The signal from the slip sensor is then processed and incorporated into the control scheme, such that the hand tightens its grip automatically whenever slip is detected. Once it closes sufficiently, the object stops slipping, and the hand returns to rest. Care must be taken in the signal processing to ensure that other vibrations, such as those created when the hand is accidentally banged, are filtered out, and only the slip signal remains. There are many ways to detect slip, process the signal, and filter out the artifacts or "noise" signals.

3.2. PIEZOELECTRICITY

The piezoelectric effect was discovered in 1880. There are currently hundreds of known piezoelectric materials. Early piezoelectric materials were made of quartz crystals and Rochelle salt [6]. When these materials were mechanically stressed, a charge separation occurred inside the material. A mechanical vibration resulted in a corresponding electrical vibration across the piezoelectric material. Similarly, a voltage difference across the material would result in a mechanical stress over the material. This effect allowed for a transducer between mechanical and electrical events. In 1947, barium titanate (BaTiO3) was discovered to be piezoelectric, followed by the observation of a very strong effect in lead zirconate titanate (PZT) ceramic. Piezoelectric polymers were discovered in 1924, but not used much until the sixties. In 1969, a strong piezoelectric effect was

seen in polyvinylidene fluoride (PVDF)[7]. This material received much use, especially in industries using ultrasonic devices, where ceramic devices were too brittle and fragile, and did not have an adequate frequency response.

PVDF and other piezoelectric polymers are produced by a technique in which the material is stretched and drawn while being exposed to a high level electrical polarization field. The origin of piezoelectricity in PVDF is not completely known, but is thought to be explained by the "dipole model". PVDF is half crystalline and half amorphous. The crystalline phase consists of a non-polar and a highly polar phase, which arrange to form dipole moments. These dipole moments exist in a random orientation. However, after being exposed to an electric field, the polymer chains become aligned with the electric field. This results in a net polarization in the material, which results in the piezoelectric response. [8]

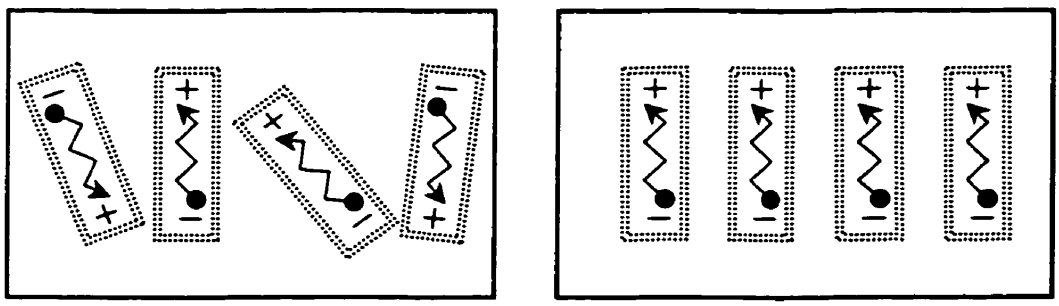

Figure 3.1. (a) Randomly oriented dipoles. (b) Aligned dipoles.

3.3. PREVIOUS WORK ON SLIP DETECTION

3.3.1 Previous Work by Warren D'Souza [1]

Initial research in slip detection at BMC began in 1994 with Warren D'Souza's Master's thesis [1]. He worked together with Aastra Aerospace in Toronto, who required the same technology for their industrial processes, which used large electromechanical grippers. Since slip detection had been investigated in the field of robotics, he researched the different ways of detecting slip that have been previously tried. These included high frequency acoustic emissions, photo-elasticity measurement using light beams, and sensing of acceleration. These methods were found to be insufficient, as they were direction sensitive and often quite complex. The method that was deemed most acceptable was the use of PZT; a piezoelectric ceramic made of lead zirconate titanate crystal, based on the work of CutKosky (1993) [18]. This would be used as a detector of the low frequency mechanical vibrations produced during slip. Piezoelectric materials are electromechanical transducers. They convert mechanical vibrations into electrical vibrations. They also work the other way; when an electrical vibration signal is applied to them, they produce a mechanical vibration. They are commonly used as microphones and speakers in applications where size is a limiting factor, since they are quite small. Because of their small size and ability to detect mechanical vibration, they are ideal for detecting slip vibrations. Note that they only respond to changes in pressure, which is vibration, but not to constant pressure. The main drawback of using these sensors was noted to be their general response to all vibrations, not just the ones created by slip. As

such, Aastra had a problem with their gripper, that occasionally it would respond as if slip was present, when it actually was not. This was a result of incidental vibrations picked up from the environment that were strong enough to be detected by the sensors, such as a jarring of the apparatus. The other drawback that was noted had to do with the materials surrounding the sensor. The sensors required a covering, for protection, and a backing. See Figure 3.2.

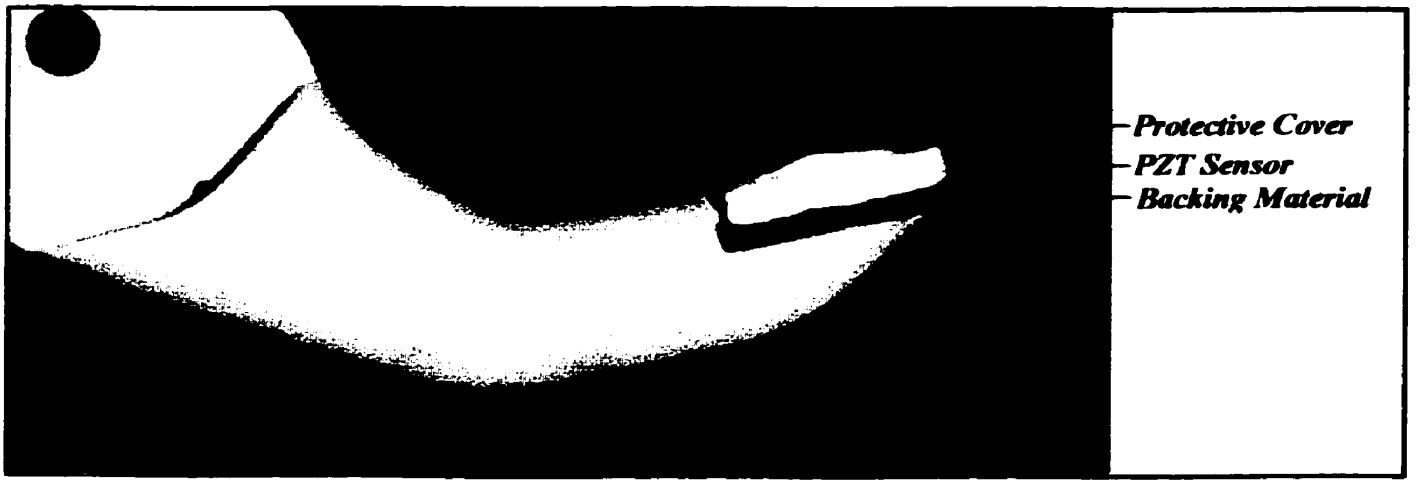

Figure 3.2. PZT Sensor, with Protective Cover and Backing, Mounted on a VASI 5-9 Finger.

Different materials cause vibrations to transmit and reflect to different degrees, especially at their interface. The optimal materials had to be determined for slip detection. Furthermore, in a myoelectric hand, a plastic glove on top of the sensor would create another layer of material that had to be taken into account.

The main work of the thesis was to determine the optimal materials for the backing and

covering of the sensor, and to design a system that eliminated the response to noise vibrations, so that only true slip was detected. This was done using a test apparatus that consisted of a VASI 5-9 hand with PZT sensors attached to both fingertips. The hand was held steady by a fixture, and a block of material was placed between the thumb and first and second fingers and then pulled out using a pulley with an increasing weight. The signal was measured together with the position of the block being held to see when slip occurred. The slip signal was filtered and converted to a digital signal. The slip signal was initially thought to be wide-band, so a broadband amplifier was used (30Hz-100kHz). Then, to reduce electromagnetic interference, a band-pass filter was used (100-1200Hz). (For a basic explanation of filtering and EM vibrations, see Appendix A). The signal was then digitized using an analogue to digital converter, sent to a desktop computer, and processed and analyzed using software [1]. The software program was written, tested and altered to determine the best algorithm for reducing vibrations due to banging while picking up vibrations due to slip. Details of the software can be found in D'Souza's Master's thesis[1]. The backing and covering materials were changed to determine the optimal combination. Rubber, silicon, nylon aluminum, steel and alumina were used for the covering material, and rubber, silicon, nylon, and aluminum were used for the backing material. It was found that soft materials worked best as a backing, while hard materials worked best as coverings. It was determined that the use of steel as a covering and rubber as a backing was the best combination out of the materials tested.

It was thought by the author that these results could be explained by acoustic impedance matching, although D'Souza does not discuss this in his thesis. Acoustic impedance is a measure of how much a material resists or allows sound waves, which are actually mechanical waves, to pass through it. Of special interest is the effect at the interface between materials. If the two materials have similar values of acoustic impedance, then sound vibrations pass through the interface. This is referred to as transmission of a mechanical wave. If the values for the acoustic impedances of the two materials are different, the sound waves partially reflect back at the interface. This is called reflection of mechanical waves.

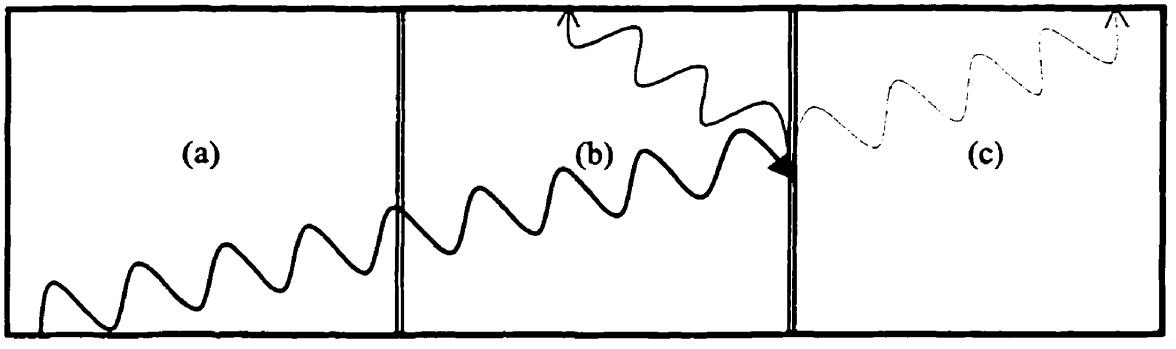

Figure 3.3. Transmission of a Wave Through Three Mediums. Medium (a) has the same acoustic impedance as (b). (b) and (c) have difference acoustic impedances.

Since PZT is a hard material, the covering would best be a hard material as well, such as steel, so that vibrations are transmitted through the material interface. However, the backing is best suited to be soft, since a soft material usually has a vastly different value of acoustic impedance than a hard one. As such, the sound waves reflect when they reach the backing interface. This impedes the waves from passing through the sensor interface

and results in a higher level of signal at the sensor, since the reflected waves act upon the sensor as well. See Figure 3.3. In this case, region 3.3 (a) would be the steel covering, 3.3(b) would be the PZT sensor, and 3.3(c) would be the rubber backing. An additional problem was caused by the cosmetic glove and the resulting acoustical impedance mismatch. Since the plastic glove is soft, vibrations reflect at the interface between the glove and the sensor covering. This resulted in insufficient signal reaching the sensor. As a result, slip could not be detected with the glove on the hand.

The other main part of D'Souza's thesis looked at the best algorithm for reducing noise. Here "noise" refers to mechanical vibrations created by a source other than slip, and not electromagnetic noise, which is easily filtered out using common electrical techniques. It was decided that the best way to distinguish between the noise and slip signals was to use the phase difference between the two signals as the identifying feature. The experimental setup consisted of a VASI 5-9 hand with two PZT sensors on the front of both fingers. Both sensors picked up slip and noise signals, but it was hypothesized that the phase relationship was different for the two signals. This idea relied on the following premise: The structure of the noise signal would be fairly identical at the two sensors, because they are picking up the same signal created by the same source. The slip signal would be significantly different at the two sensors, because the object is not slipping in exactly the same fashion at both fingers. As a result, the phase difference between the signals from the two fingers should be constant for a noise signal, and varying for a slip signal.

The signals were processed and sent to a computer. A program was written to implement the noise cancellation algorithm that was similar to a digital version of a phased locked loop[1]. The program took a sample of the two signals in a period of time. This time window allowed manipulation of the two signals. One signal was held constant, while the other was moved backwards and forwards in time. This was done until the signals from the two windows matched up. In the case of noise, it was expected that the windows would match up quickly, and result in no phase difference between the signals. In the case of slip, the windows would never quite match up, due to the difference in the signals, and the result would be a varying phase difference between the two signals that would never settle at any point. If any phase difference was present, this would create an "error" signal. This error signal would be "on" most of the time during slip, and "off" most of the time when noise was present. However, it would take some time even for the noise signal to match up, so some error signal would always be present. Also, the slip signals would match up occasionally and produce no error signal. Therefore, the error signal was averaged over a certain time period to take these factors into account. If an overall error was present in that time period, that is, if the amount of error signal was over a preset threshold number, then a slip signal would be sent out to the motor, which would then proceed to close the hand. This was the basic routine carried out in the experiment, and several factors were changed systematically to find the best combination. These included using the slope of the signal as the input, using the slope and the curvature of the signal as the input, using different filters, varying the size of the time window, and

varying the manner and speed in which the windows shifted with respect to each other. It was found that the only significant improvements came from comparing the second derivatives of the signals, in addition to slope matching, and by "scaling" the error signal. "Scaling" was a method of adding a certain mathematical gain function to the signal that, in effect, amplified the slip signal more than the noise signal, and as such increased the SNR. The results showed that using "advanced" window matching algorithms that attempted to anticipate and compensate for phase shifts did not help reduce noise. As such, it was concluded that the most basic window matching algorithm should be used. Since the aim of this project was proof of concept, the test results were used for implementation in an actual prosthetic hand, using the best materials and algorithm found. The signal from the sensors was sent to an analogue filter and an analogue-to-digital converter. The output then went to a personal computer, where the programmed algorithm ran, and then to a motor system. To simplify operation, the small, highly geared motor (1:1000) in the original hand was replaced with a simple low gear ratio motor (1:3), which was thought by D'Souza to give a more linear response than the original VASI motor and gear system. Less gearing meant less output grip force, so a larger motor had to be used to compensate for this. A prototype of the complete, closed-loop system was tested with and without the use of curvature matching in the signal processing, to verify that curvature matching indeed improved the performance of the completed, closed-loop system. The concept of using slip detection in a child-sized prosthetic hand was thus shown to be feasible.

D'Souza's thesis concluded by recommending points for future work that would need to be addressed before slip detection could actually be implemented in commercially available hands. The first concern was the motor and gear system. It was noted that the original small, highly geared motor that is used commercially in the VASI 5-9 hand would have to again be used in the final system. In addition, the algorithm found was not thought to be a complete solution. It was thought that further development might yield better results in discriminating between slip and noise. Further research was suggested for the interface and backing materials of the sensors. Testing with human subjects would be needed in which a variety of objects would be lifted to determine any remaining inadequacies of the system. Finally, a complete miniaturization of the design would be needed so that the control circuitry could fit within the available space in the VASI 5-9 hand, which is 25 mm x 38 mm x 10 mm (9.5 cm^3) [27], rather than running off a personal computer, which, even in the best case, would be prohibitively large in a clinical application.

3.3.2. Previous Work by Kathleen Surry [2]

The slip detection project at BMC was continued by Kathleen Surry in her Master's thesis after Warren D'Souza left [2]. She reworked the previous computer program so that it was modular and simplified. This was done to ease electrical implementation and miniaturization. The entire experimental setup was then rebuilt and re-tested in order to verify the previous findings. The issue of motor interface was looked at, and a motor

control circuit was implemented such that it interfaced with the pre-existing motor control board in the VASI 5-9 hand (see Appendix F). This allowed the slip signal to be incorporated into a pre-existing hand. The overall changes implemented brought the design closer to being implementable in a clinical setting. Recommendations for future work were made regarding the following issues. It was deemed necessary that the slip detection system be functional with complaint fingertips and with the cosmetic glove on. The problem lay in matching the hard PZT sensor with the soft complaint fingertips. Several suggestions were made, including using viscoelestic materials, changing the mechanical design of the sensors' location and complaint fingertips' shape, or using sensors attached to the glove. The next step needed would be miniaturization of the controller and surrounding circuits. Then a testing protocol would need to be devised for clinical testing. Finally, the issue of power supplies would need to be explored, that is, whether the added slip system would increase energy drainage, and if so, a supplementary means of supplying power would need to be investigated.

3.4. Otto Bock's Slip Detection System

There is a German based company called Otto Bock with an office in Canada* who released a new prosthetic hand last year that incorporated a slip detection system. The slip detection technology is called SUVA, named after the institute that helped develop it.[24] Otto Bock is a relatively large prosthetics company with a worldwide clientele. They

* Otto Bock Orthopedic Industry of Canada Ltd. Oakville, Ontario, Canada.

offer a wide range of prosthetic devices, including myoelectric hands for adults and children. Clients at BMC often order prosthetics hands from Otto Bock. Many accessories, such as myoelectric sensors and batteries are ordered from Otto Bock and used as industry standards. Their new line of adult prosthetic hands comes with the slip detection option. It was not determined whether the new system was only available in adult hands because of any design limitations, or for what reason it was not made available in child-sized hands at the time of this writing. No specific technical information was made available after request by the author at the time of writing, but a chance did arise to test this hand's performance, as it was available for a short time when a customer ordered this hand through the myoelectrics department at BMC. There was only enough time to test the hand qualitatively.

The Otto Bock hand's slip detection system was tested to determine the state of the art in slip detection, as it is the first commercial available slip detection system for prosthetic hands, and Otto Bock is a very prominent, leading company in myoelectrics.
The hand came with four options for control. These had to do with the user's ability, muscle strength and coordination. There was time to test two of these settings. Myoelectric sensors were attached to the author's forearm flexors and extensors and were used to control the hand during testing. The adult hand was advertised to be capable of producing 100 lbs of force at full strength. Because of this, there was a warning in the manual to be careful during sensitive tasks, such as shaking hands, during which the slip system could activate and crush the other person's hand. By contrast, the VASI 5-9 hand

produced about 15lbs at maximum pinch force, which is about as much as a natural adult hand can produce. The control options came as coloured pins that were inserted into a slot in the hand, with an option for the slip system to be turned off. One option was full function for a user with two strong muscle sites, allowing them to open and close with proportional control. This setting was tested several times by placing an object within the grasp and slowly pulling it out to see how the hand behaved. The object was a long plastic cylinder that was deformable, so increased pressure would be visibly detectable. The motor also emitted a beeping sound when activated. These auditory and visual signals were used to determine whether the slip signal was working. There was no detectable response to slip or banging noise after repeated trials with this control option.

Another control option was tested. This one was of particular interest because it partly implemented a form of the grasping algorithm intended for the design described in this thesis (see Section 2.7). This design was meant for users with only one available muscle site. The hand remained fully open in the resting stage, and when the user sent a signal from the muscle, it would begin to close. When the signal stopped, the hand would fully open again. There was an option of keeping the hand in a closed position by performing a certain muscle contracting pattern. The key feature of interest here was that the hand would automatically stop closing once it detected a grip force of 10lbs. After this, the slip system would activate and respond to slip by closing. This is similar to the author's design as described in Section 2.7. The hand indeed functioned as advertised. It closed on an object, but would stop closing once a grip was established even in the presence of a

muscle signal. The slip system in this case worked, as the hand was observed to close when the object was moved inside the grasp. However, the movement had to be slow and steady to elicit a response. The hand also responded equally well to banging. If the hand was banged, or lightly flicked with a finger, the motor was activated and the hand closed on the object. In this test, the Otto Bock hand's SUVA-sensor system was not immune to noise.

3.5. SLIP RESEARCH OUTSIDE OF BMC

The issue of slip detection was looked at in the robotics industry in the past. This was needed in robotic hand manipulators used in industrial processes, as well as in tactile sensing for robotic hands. Most of the results and innovations made in the robotics industry were unusable in this project because they used complex sensors that were housed in relatively large sized hands (compared to a child-size prosthetic hands), had no glove covering, and were line-powered, with a computer controller and signal processor. This situation allowed for much fewer limitations and design constraints. As such, many of the robotics solutions are highly impractical in a child-sized myoelectric hand setting where size, power, and degree of signal processing are very limited. D'Souza (1996)[1] investigated possible options for slip detection technology and found piezoelectric sensing to be ideal for this application. The author agreed with this finding upon investigation, but also looked at the recent literature to investigate any new research developments in the field of slip detection in prosthetic hands.

One recent article on detection of slip using neural network processing was published by a group from Italy headed by De Rossi (1998) [13]. Although the results were encouraging, they are inapplicable to this project. For one, they used neural network processing that requires a large amount of computing power, and their method was dependent on a slip sensor that detected shear stress at the sensor surface. With a myoelectric hand, there would be a glove on top of this, and the sensors would likely not work properly.

Another recent article was published by Tura *et al* (1998) [14], in which a sensory control system for an upper limb myoelectric prosthesis was designed and tested. The slip detection system used an optical sensor to detect motion at the fingers' surface, and an FSR (force sensitive resistor) based system to detect pressure. They implemented a form of grasping algorithm similar to the one described in Section 2.7. They gave support for the viability and usefulness of such an algorithm, but concluded that much work would be needed to miniaturize the slip detection system so that it could be installable in a prosthesis. Also, an optical system would not work with a glove on top of it. In their analysis, they dismissed the use of "piezoceramic" sensors "for problems of fragility" [14]. This problem would not exist had they considered a piezoelectric polymer.

Another prosthetic hand that had been described in the literature is the Southampton hand[28], which is actually an ongoing evolution of hands that began in 1969 at the University of Southampton. The most recent design is the third generation, four degree of

freedom Southampton Adaptive Manipulation Scheme hand [20]. The hand uses force sensors and acoustic slip sensors to detect contact with an object. This sensory information is processed by a computer that decides on the best grasp for the situation. The hand has an adaptive grasp, and uses four motors [28]. While this hand is academically interesting, it is questionable whether it could be clinically applicable. Its mechanical design and control system are complex, and would be probably not be very robust in a rough, real-life environment. It does however show promise, and a future version of the hand might indeed become the standard in myoelectric hand design.

3.6. SUMMARY

After reviewing the available information on slip detection and analyzing the previous work, several conclusions were reached as to the direction of the project. First of all, the design considerations were outlined. They are summarized in Table 1. on the next page.

DESIGN CONSIDERATIONS

- Address major previously identified problems and provide effective solutions
- Simplicity
- Ease of incorporation into an existing product
- Use of common, easily available and inexpensive parts and processes
- Power consumption low enough that a rechargeable 6 Volt Otto Bock battery rated at 270 milliAmp hours could power a VASI 5-9 hand with the slip detection system for one entire day and be recharged at night
- Small enough size and weight that the control circuitry could be contained within the VASI 5-9 and be built on a circuit board that is less than 9.5 cm^3 in size.
- Robustness- at least a one year life span, requiring no more care than an initial set-up and routine annual maintenance.

Table 1. Design Considerations

These considerations led to the experimental approach and setup. Piezoelectric sensing was chosen to be the best, most robust, and simplest method of slip detection. However, the use of a ceramic was thought to be a problem, as it led to many limitations, such as fragility and the need for a cover and backing, and incompatibility with compliant fingertips and the cosmetic glove. Because of this, a different type of piezoelectric sensor was sought, and a simple, yet effective way of processing the signals was desired.

4. EXPERIMENTAL DESIGN AND METHODS

4.1. SENSORS

The next step in the design process was a very critical one, as it would allow for the use of compliant fingertips with the slip detection system. This step was the choice of sensors. The previous sensors used were PZT piezoelectric ceramic sensors [1, 2]. These were made of a hard material, about a centimeter thick. The fingertip was cut so that the sensor could be placed on the finger. See Figure 3.2 on page 30. While it was believed that the choice of piezoelectric sensors was a sound one with regards to the method of detecting slip vibrations, it was thought that another type of piezoelectric sensor might work better, since PZT is so hard and brittle. Investigation led to the finding of another commonly used type of piezoelectric material, the piezoelectric polymer. While many polymers have piezoelectric properties, polyvinylidene fluoride, or PVDF, is the one with the greatest sensitivity. The US manufacturer, AMP*, which later sold their sensors division to MSI**, Measurement Specialties Incorporated [25], claimed that the PVDF sensors had many features that made them better than ceramic piezoelectric devices.

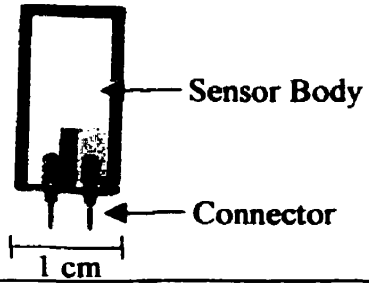

Figure 4.1. PVDF Sensor

* AMP Sensors. Valley Forge, PA, USA. (Bought out by MSI)

** Measurement Specialties Incorporated. Fairfield, NJ, USA.

See Appendix B for specifications provided by AMP detailing values for PVDF physical properties, including thickness, piezo strain and stress constants, capacitance, Young's modulus as well as additional physical quantities.

In Table 2, AMP compares some physical properties of PVDF sensors to PZT and $BaTiO_3$.

Property	Units	PVDF Film	PZT	$BaTi0_3$
Density	10^3kg/m3	1.78	7.5	5.7
Relative Permittivity	$\varepsilon/\varepsilon_o$	12	1,200	1,700
d_{31} Constant	(10^{-12})C/N	23	110	78
g_{31} Constant	(10^{-3})Vm/N	216	10	5
k_{31} Constant	% at 1 kHz	12	30	21
Acoustic Impedance	(10^6)kg/m^2-sec.	2.7	30	30

Table 2. Comparison of PVDF sensor properties with PZT and $BaTiO_3$.[26]

AMP claimed that these sensors have a voltage output orders of magnitude higher than other types of piezoelectric sensors. This can be seen by comparing the value for g_{31}, the piezo stress constant, to PZT and $BaTiO_3$ in Table 2. It is can also been seen in this table that PVDF has a lower density and acoustic impedance than PZT and $BaTiO_3$.

In this project, the relative output of the original ceramic PZT sensors was tested against the PVDF sensors. Both sensors' outputs were connected directly to an oscilloscope where their output levels were compared using common input signals. Both raw outputs were in the mV range. The PVDF sensors were found to have an output between 10 to

25 times larger than the ceramic PZT sensors, which confirmed the manufacturer's claim that PVDF sensors produce a higher output level than PZT.

The capacitance of the PVDF sensors was measured by the author to be 500 ± 50 pF., which is in agreement with the advertised value of 485 pF [26]. The capacitance of the PZT ceramic sensor is almost too small to be measured, at approximately 50 pF. This means that the PVDF sensor has a capacitance that is at least an order of magnitude higher than the ceramic sensor. This is due to the extremely low sensor thickness (28 μM) achievable with PVDF. Capacitance is inversely proportional to a parallel plate capacitor's thickness, and the sensor effectively acts as a parallel plate capacitor in series with an alternating voltage (AC) source. See Figure 4.2. The internal capacitance of the sensor means that it acts as a high pass filter when driving a load. This makes physical sense, as the sensors only respond to a vibrating mechanical input, and not a steady pressure. A higher internal capacitance results in less capacitive reactance, and thus a greater low frequency response, and an overall wider bandwidth. Since slip is a low frequency signal, a greater low frequency response would mean a higher level of slip signal. As such, it stands to reason that the PVDF sensor would be more sensitive to slip vibrations than the PZT sensor, since the PVDF sensor has a higher capacitance.

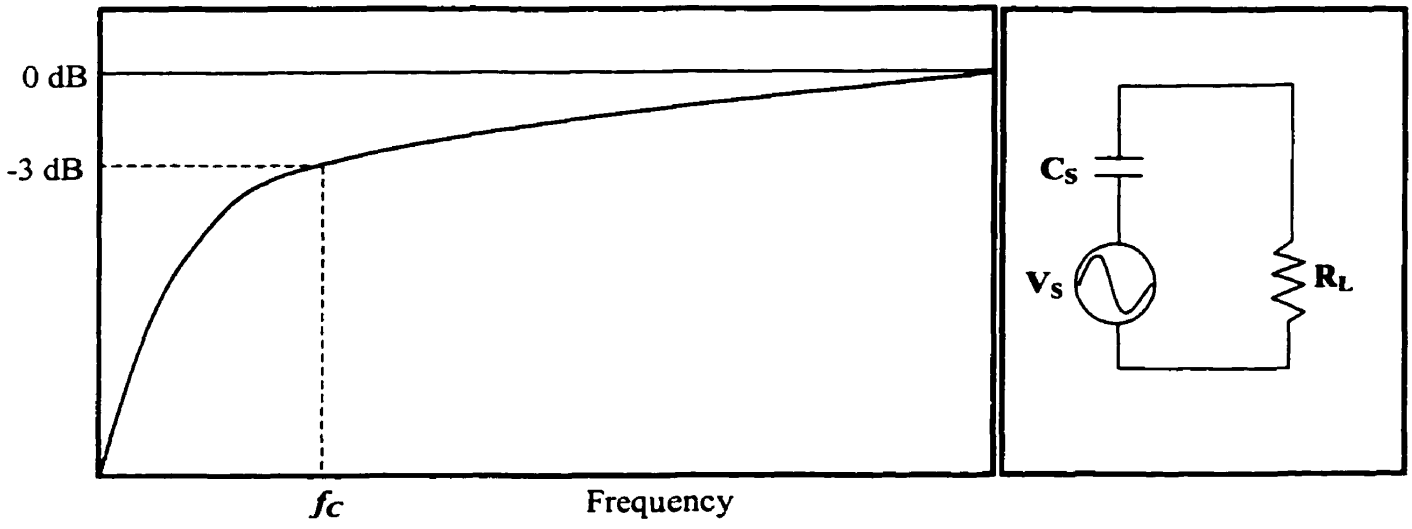

Figure 4.2. High Pass Filter Characteristics of Piezoelectric Film.

In Figure 4.2, the frequency set by the 3 dB point can be found using the equation:

$$f_C = Cut\text{-}off\ Frequency = 1/(2\Pi \bullet R_L \bullet C_S) \qquad \textbf{\textit{Equation 1}}$$

The main attraction to the PVDF sensors was their small size and thinness. They were claimed to be paper thin, which made them very flexible, because the material is, fundamentally, a plastic polymer. This latter property was the main reason for their selection. The thin sensors could be glued onto the surface of the finger, so that the hand need not be cut out to make room for them as with the ceramic, and no backing and covering material would be needed, as they are self-contained sensor units. The second main reason for using PVDF sensors was that since they are so flexible, they could be used with compliant fingertips simply by placing them on top of the compliant fingertips. They bend and flex together with the fingertips, unlike the ceramic. The final reason for using these sensors was that of acoustic impedance matching, so that the system would be

compatible with the plastic glove covering. The glove is made of PVC, polyvinyl chloride. This material is chemically similar to PVDF, both are soft and rubbery, so it stands to reason that the two have similar values of acoustic impedance. As such, there would be a close matching at the glove-sensor interface, and significant signal transmission through the interface with minimal reflection. This would lead to the slip system working with the addition of the PVC cosmetic glove, as in fact was later observed and verified (see Section 5.7). With the ceramic sensors, there was acoustic impedance mismatching at the glove interface that led to significant and detrimental slip signal loss. Using the PVDF sensors was thought to raise the amount of signal reaching the sensors because of acoustic impedance matching, and, as such, increase the overall signal-to-noise ratio when it would become crucial to get as high a level of slip signal as possible.

In summary, the choice of PVDF sensors was based on the issues of compliant fingertip and cosmetic glove compatibility, and provided an inexpensive ($1 each), and easily applicable sensor solution.

The next stage in the project was to design and build the electronic control circuitry. This involved considering the theoretical aspects of slip noise cancellation, as well as dealing with issues of circuit design.

4.2. SENSOR PLACEMENT AND MODIFICATION

Initially, the sensors were placed at the front of both fingers, following the design of D'Souza (1996). Later, another two sensors were placed on the back of both fingers. These positions were tested for effectiveness and, in the final design, for reasons detailed in Sections 5.3-5.6, a sensor was mounted on the thumb with a compliant fingertip. In this last configuration, another sensor was placed on the thumb back. The reasons for this will be discussed when the progression of the noise cancellation circuit is outlined in Section 5.6.

The sensors were physically processed before being glued to the finger. It was found that the sensors had a protective plastic layer on them, and by very carefully peeling off the protective layer, the sensor could be made even thinner and more flexible. The actual sensor then consisted of the PVDF layer, with two metallic foils on either side.

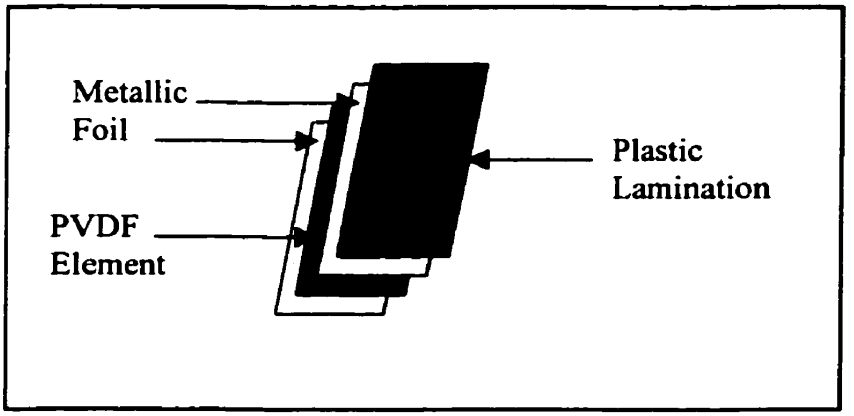

Figure 4.3. Layers of the PVDF Sensor

The entire outer border of the sensors was trimmed to reduce size, as they were a few millimeters too big for the finger. See Figure 4.1. It was important not to cut the actual sensor area in an effort to reduce their size, as this would sometimes cause the metal films to touch each other, thereby shorting out the sensor irreparably. In addition, sensor placement was made difficult by the fact that the finger had a bi-convex surface; it curved in two dimensions. This caused the sensor to pinch and fold on itself at the point where the two curves intersected. To compensate for this, a small slit was cut at the bottom of the sensor between the two connectors (see Figure 4.1), before the metalization began (the metalization is the lighter region in the sensor's interior). This allowed the two flaps to separate at the point of curve intersection and prevent distortion of the sensor.

The sensors were glued onto the fingers with cyanoacrylic glue (crazy glue). The thumb sensor was glued on with silicone, the material used for the compliant fingertip. Joiner (1994) [3], who researched compliant fingertip materials, chose this material as the ideal one for compliant fingertips. It performed well in the slip detection project, and was inexpensive and readily available. A thumb with the frontal cavity dug out was used and filled with silicone. The sensor remained attached to the silicone, and was able to bend and conform to the fingertip. Silicone grease was used between the sensor and the glove to ease placement of the glove onto the finger, as this was a tight fit. In addition, the silicone grease served to reduce any air gaps between the glove and the sensor, thereby increasing the area of contact, which led to a higher sensor output signal. It also provided a medium of transmission that was acoustically compatible with the soft glove, sensor, and silicone fingertip.

Another type of sensor attachment was tried, which proved unsuccessful. This was the attachment of the sensors directly to the inner surface of the glove, instead of to the body of the finger. Cyanoacrylate glue was used, which did not work well. The sensors and attaching wires were glued to the glove. Upon drying, the glue became too stiff in comparison to the glove. The glove had to be inverted to attach the sensor, and upon re-inversion, the wires attached to the glove snapped and broke. This problem was discussed with members of the electronics department at BMC, and it was learned that attachment of wires to a glove has been an ongoing, unsolved problem for them [27]. Therefore, it was decided that to build this type of design would be too complicated an undertaking, and it was abandoned, since one of the design criteria was simplicity and ease of construction. This design may be a viable solution in the future if an easy and robust way of attaching wires to the inner glove is developed.

Another design was attempted that was a variation on the sensor in the glove. The idea for this came when it was observed that the tip of an oscilloscope probe acted as a weak mechanical vibration sensor, with an output similar to the piezoelectric sensors. It was thought that this was due to the plastic material of which the probe lead was made. The plastic material may have had some piezoelectric properties, and the probes were constructed such that there were metal plates surrounding the plastic, which would effectively measure the piezoelectric voltage produced. Upon further research, it was found that most materials indeed have some degree of piezoelectricity. The cosmetic glove was made of PVC, a weak piezoelectric material. Therefore, it was proposed that

the glove could act as a slip sensor. This could be done by applying a thin, conductive coating of metal to the inside of the glove. The metalization would act to detect the piezoelectric charge. With this design, no sensor would be needed, just a metal layer, as the glove material itself would act as a sensor. Since the glove would be the sensor, any slip vibrations on the glove surface would be picked up without attenuation. Vibrations coming from the body of the hand would be less at the glove, and this may act as a suitable acoustic division needed for increasing the SNR of slip to noise. This design failed for the same reason as the previous one. The fingers were inverted, and upon re-inversion, the metalization cracked and chipped off. Nickel enamel paint and a silver epoxy were used for the conductive metal material. This design did not seem very robust, and would be liable to breakdown in daily use. Its only viability would lie in finding a simple way to attach a conducting layer to the inner glove surface. No satisfactory method was found in this investigation.

Note that attaching the sensors to the outer surface of the glove was never a viable option because of wear. This design would not be robust because daily use would degrade and deteriorate the sensors, and they would need to be replaced often. One of the main reasons for having a glove is for protection of the hand, and it would also act to protect the sensors. Otherwise, some sort of protective layer would still be needed on top of the sensors, preventing direct contact with the sliding surface. In either case, adding sensors to the glove would not be found acceptable by clinical prosthetists, unless a very unobtrusive, robust, and unseen device was used. Because of this constraint, the only signal available was the one that traveled through the glove surface and required a high

level of amplification, which always leads to higher noise. This is because noise is always present at low levels, and the weaker the signal, the higher the level of amplification that is needed. Hence the noise became a more pronounced part of the overall signal since it too was amplified, thereby lowering the SNR.

4.3. INPUT/OUTPUT DEVICES AND FREQUENCY RESPONSE

Because of the PVDF sensor's high sensitivity, it picked up all sorts of vibrations other than slip. Most of the EM interference was seen at 60 Hz, which is the power line frequency. This type of noise was reduced by using a basic band-pass filter centred at 400 Hz with a Q value of 10. The other types of noise came from external vibrations, produced by banging the hand, banging the table that the hand sat on, or by bringing a vibrating speaker near the hand. The first method looked at in an attempt to isolate slip signals from noise was separation on the basis of frequency. The sensor output was recorded by a spectrum analyzer for both slip conditions and noise conditions.
Both signals appeared to be broadband, with no particular frequency characteristics. Furthermore, both signals' band ranges were similar, in the lower end of the spectrum, at around 120-1200 Hz. Figure 4.4 shows the spectrum analyzer output from a sensor attached to the back of the VASI 5-9 hand's forefinger. Figure 4.4(a) shows the output with no signal. The top trace in each graph is the spectrum analyzer in the region between 0-1000 Hz, and the bottom trace is the oscilloscope output. With no external signal, the largest signal seen was the 60 Hz power line, shown on a normalized scale as a spike in the left region of the graph. Figure 4.4(b) shows the output for a banging noise

signal. The VASI 5-9 hand was placed on a table and the table was banged three times. Each bang can be seen as a spike in the lower, oscilloscope trace of the graph.

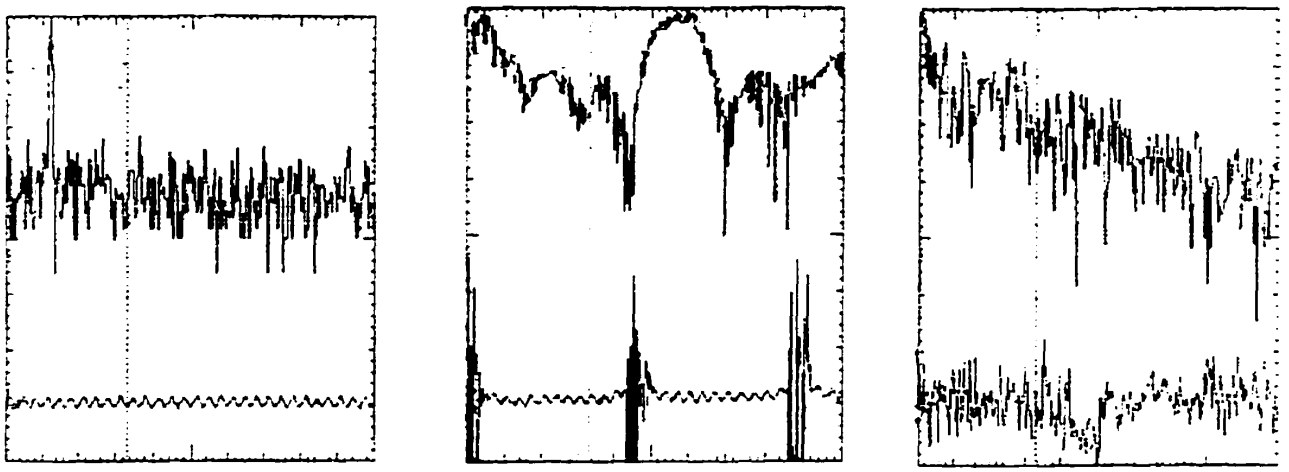

Figure 4.4. Spectrum Analyzer Outputs on a Normalized Scale, 0 – 1 kHz (Top trace). Sensor Output (Volts) vs. Time (Bottom trace). a) No Signal. b) Noise. c) Slip.

Figure 4.4(c) shows the output for a slip signal. The signal was create by having the hand grip a table edge, and then sliding the hand along the edge.

Higher characteristic frequencies were searched for on the spectrum analyzer, up to 1 MHz, but none were found. This feature made it impossible to reduce this noise on the basis of frequency alone. This left two other basic waves characteristics to be used as a basis for noise reduction: amplitude and phase difference.

The outputs of both sensors were analyzed, this time on an oscilloscope. There was one sensor on the back on each finger. The inputs were a slip condition and noise. Noise was created using a speaker at a set frequency. This was a practice repeated often in this project to replicate noise. The reason for doing this was that the speaker output, which

came from a signal generator, was of constant amplitude and of a single frequency. In this way phase could be looked at, independent of variations in amplitude and frequency. It was also a means of generating a repeatable signal, which was needed for quantitative analysis. It was seen that the amplitude difference between the two sensors varied more for slip than for noise. In both cases, a phase difference was seen between the two sensors, as shown in Figure 4.5. This led to the general approach on how to separate noise from slip. Note that from here on "noise" indicates noise from external physical sources such as banging, and not EM noise.

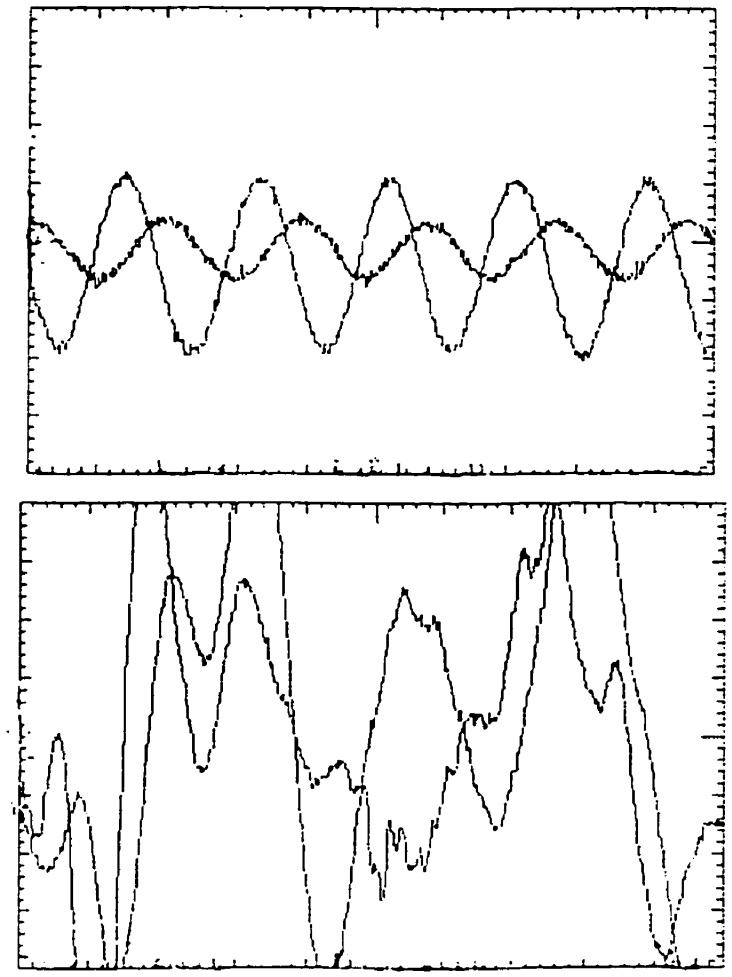

Figure 4.5. Phase difference between sensors for slip (bottom) and single frequency noise (top). Scale: y-axis 20mV/Division, x-axis 500 μs/Division

4.4. NOISE CANCELLATION ALGORITHM-GENERAL APPROACH

It was thought that noise could be reduced by two means: using the amplitude difference and the phase difference between two sensors at different locations. The amplitude difference could be used as an indicator for slip by measuring the difference between the two sensor signals, on condition that there be a greater difference of amplitudes in slip signals than in the noise signals. If the signal gains were adjusted so that the signals were equal for noise at both sensors, subtracting the adjusted amplitude values would yield zero output for a noise input, and a measurable output for a slip input. This is effectively common mode rejection. A similar approach could be used for phase difference. If the phase shift between the two signals was electronically adjusted so that it was zero during the noise condition, there would likely be a measurable phase shift during slip. This would depend on the phase shift being different for both input cases, which is a reasonable assumption, for both differences in amplitude and phase between the two sensors. The reasoning behind this has to do with the physical signal paths in the two conditions. For noise, the source is external and localized. This means that the noise vibration will travel approximately the same distance to reach both sensors, and through the same medium. Except for small variations in the sensors and hand material, the noise signal should be the same at both sensors, having roughly the same magnitude and phase at both sites. However, for slip, the signal is generated at two different sites for each sensor, one at each fingertip. Therefore, the signal would probably have different magnitudes at each sensor. A similar argument can be made for the variation in phase

between the two sensors. Therefore, by subtracting the two signals' phase or amplitude values and then zeroing the output in reference to a noise signal input, a slip signal input should produce an output that is immune to noise. Of course, for this to work, the basic assumptions have to be met that there is in fact a repeatable difference in amplitude and phase shift between the slip and noise conditions. However, if the basic conditions do not hold, it might still be possible to create them by manipulating the physical system, such as through the addition of compliant fingertips, and by using strategic sensor positioning. To do this, the basic properties of the mechanical system of the hand would need to first be investigated

4.5. BASIC CIRCUIT BUILDING BLOCKS

The circuits were divided into basic blocks that were then cascaded to provide the desired combined effect. This allowed each circuit to be designed, tested, and troubleshot individually, to make sure that it works properly on its own before using it in the combined circuit. Many options were available for each circuit, and the choice was made based on simplicity, functionality, performance, component availability, and expense. For circuit diagrams, see Appendix G. The central circuit was the instrumentation amplifier (IA). This circuit was used to perform the "subtract" function. It consisted of three operational amplifiers in an integrated circuit (IC) package with an inverting and non-inverting input. The output was the difference of the two inputs, times a gain factor. After investigating different IA brands, the IA made by Linear Technology* was the

* Linear Technology Corporation, Milpitas, CA, USA.

chosen, because it was a precision, micro-power CMOS device, and allowed for two preset gains of 10 and 100. (See Appendix D for full specifications)

An operational amplifier was used to make a split power supply with a ground at the midpoint value between positive and negative, so that the IA and other circuits could be run with a single power source, which was usually a nine volt battery, but sometimes a plug-in power supply or a rechargeable six volt Otto Bock battery.

The next circuit block needed was a variable frequency band-pass filter. Four second-order filters were built with a frequency range of 100- 1100 Hz (see Appendix G). Running the signal through the band-pass filter greatly reduced the bandwidth of the output, giving it a purely sinusoidal appearance. Next, four variable phase shift circuits were built. These were active circuits, which had a constant gain independent of phase. Each one was capable of providing a phase shift of 180 degrees, so two in series were used to provide a full 360-degree shift. (see Appendix G)

4.6. ANALOGUE VS DIGITAL

At this point it is worth discussing why the choice was made to proceed with analogue signal processing instead of digital signal processing. Of course, the first instinct might be to choose a digital solution using a small microprocessor and write the processing sequence as a program, as was done in previous work. The reasons analogue technology was preferred over digital processor based technology were the following: An analogue

circuit would operate faster by its very nature, since digital commands take time to execute and each step in executing a program puts in a small time delay. Here, digital refers mostly to processor based digital processing, and the delay time would be dependant on the processor speed and the length of the program. The PIC processor used in VASI hands runs at 4 MHz [27]. The required response time to slip would be in the order of milliseconds. Therefore, if the programmed processing algorithm was longer than about 1000 instructions, the time delay in the slip detection system would be critical, and would put a limitation on the response time of the system. In this application, a quick response time would be needed to respond to slip before object movement occurred. An analogue circuit is also easier to implement, and is simpler to design. If a digital solution were later desired, it would be easy to translate analogue commands into the digital language, since most functions are simple mathematical ones. To go from a complex digital solution back to an analogue implementation would be more difficult. As such, it is not suggested that an analogue solution need be the final one, but that it be the starting point, which, if later desired, could be digitized and written into a processor-based program.

5. RESULTS AND DISCUSSION

5.1.THE MOTOR

The first issue that needed to be addressed was the motor. Its internal characteristics had to be experimentally determined to see its effect on the overall slip detection system. In this sense it was not the motor alone that was looked at, but the entire gearing system that connected the motor to the fingers. The motor connected to a gearbox, which connected to several other gears, and finally to a cam connected to the fingers that caused them to rotate open or close. See Figure 5.1. The overall gear ratio was about 1:1000.

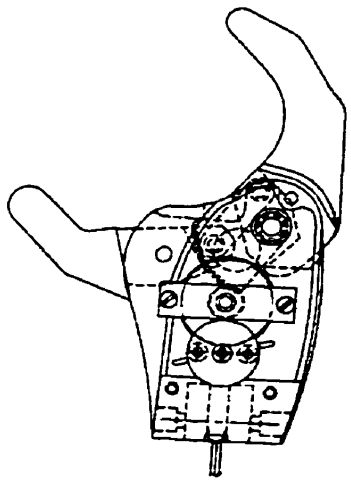

Figure 5.1. Motor Gear Diagram

Here the term high gear ratio refers to a gear train that converts high speed to high torque. The motor was a high-speed variety that turned at 12,000 RPM. The large gear ratio was needed to convert its speed into torque. The mechanical design of the fingers on the cam pivot results in a useful property of the hand. Once the hand was closed part way, applying an external force to the fingers could not cause them to open again. Conversely,

an external force could cause the hand to close. This locking mechanism was deliberately designed into the hand. It was a useful property because once the hand closed upon an object, power could be turned off, and the grip would be maintained. No more force from the motor was needed to maintain the gasp. In effect, the hand locked closed at that point. While useful in practice, D'Souza (1996) [1] surmised this property to overcomplicate his design, and replaced the motor and gearing with a simpler one. His motor had a low gear ratio and no locking mechanism, so that the output was linear. That is, the signal applied to the motor was directly proportional to the grip force. If no signal was present, the grip force was zero, and there was no locking.

To determine the characteristics of the motor unit, an experiment was conducted to test he relationship between grip force and current applied to the motor. Current was chosen as the variable electrical property, since a direct linear relationship between current and motor output was expected. This was because the relationship between current and rotational force produced by a DC servomotor is linear, and the relationship between the transmission gears is also linear. A VASI 5-9 hand was used together with an orthopaedic grip force measuring device which read from 0-60 lbs. This was more than necessary since a human hand can grip with only about 15 lbs., and child prostheses are designed to grip with even less force than this. The pinch gauge was a device commonly used at BMC to measure the grip force of different hands, and could be read to within ±0.2 lbs., which was sensitive enough for this experiment. A power supply was used which allowed both current and voltage to be limited. In this case, it was the current that was limited. The hand was placed around the grip force measuring device, and the current was slowly

raised in small increments. The subsequent change in grip force and the corresponding current were then recorded. Care was taken not to raise the current too high as to burn out the motor, by keeping the maximum current below 3 Amps.

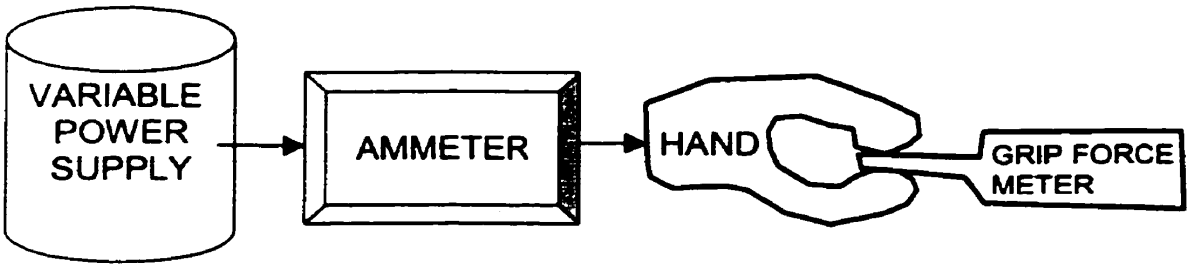

Figure 5.2. Grip force vs. current experimental setup

Three trials were conducted and all gave similar results. The results are shown in graphical form in Figure 5.3. The three graphs are superimposed on each other. The graphs were obtained by connecting the data points; no fitting was done. The reading error for the pinch force was ± .2 lbs., and for the current it was ± .005 A. There was a minimum current, below which the hand did not move. The current was slowly raised, and at small intervals the output force would jump from one value to the next; i.e. once the hand began to move, it also took some time for it to stop again. This phenomenon did not always occur measurably, and the results were the same in either case.

The graph in Figure 5.3 outlines the first characteristic of the motor, called a "dead-zone". This is a region near the origin, where current is being applied to the motor, but the output grip force is still zero.

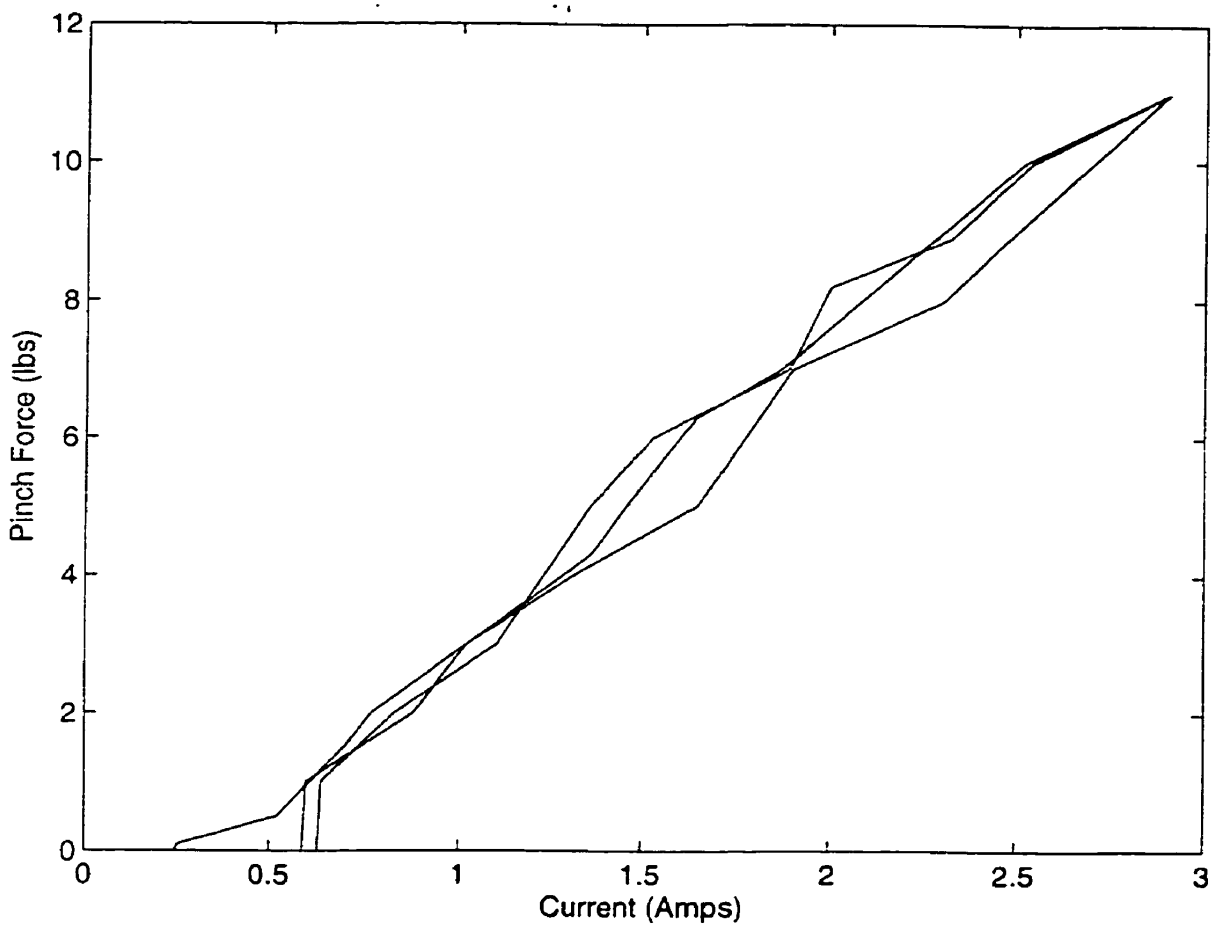

Figure 5.3. Grip Force vs. Current Graph.

The reason for the dead-zone is backlash and slack caused by the gears. A certain amount of force is needed to overcome backlash before movement occurs, and since there is so much gearing after the motor, some force had to be exerted before any movement was seen at the fingers resulting in grip force. The relationship was seen to be linear after the dead-zone.

The second characteristic of the motor system was hysteresis. This refers to the mechanism of the "locking" system. The graph in Figure 5.3 was obtained by

incrementally increasing the grip force. However, to open the hand again, the current had to reverse polarity before any finger movement was seen. When decreasing current after initially increasing it above zero, the grip force did not change until the current passed the negative region of the dead-zone. Then it opened a bit. Although the movement was small, it appears as a sudden drop to zero in grip force as the object was released from the grip. The hysteresis behaviour is shown in Figure 5.4.

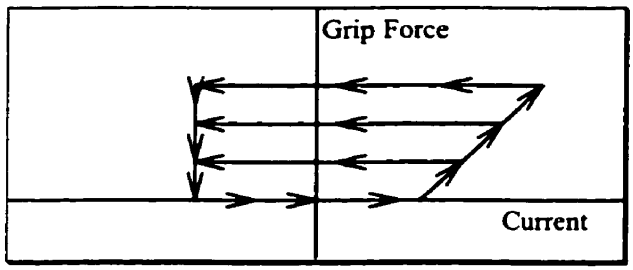

Figure 5.4. : Hysteresis in the Current vs. Grip Force.

Furthermore, it was seen that pulses of current were able to close the hand more effectively than a steady current, thus reducing the effective dead-zone. This is probably because the motor uses an internal coil of wire used as an electromagnet, and when the current is pulsed, the magnetic field produce by the coil is stronger, since a larger change in current, such as a pulse, produces a larger magnetic field. The VASI motor controller, in fact, uses pulses to control the motor. The duty cycle of the pulses is varied to change the motor output. The output frequency of the pulses is programmable, and is usually set at 22.2KHz [27]. Figure 5.5 shows an example of varying duty cycle. In the first half of the graph, the duty cycle is about equal, or 1:1. In the second half of the graph, the duty cycle changes and becomes more uneven.

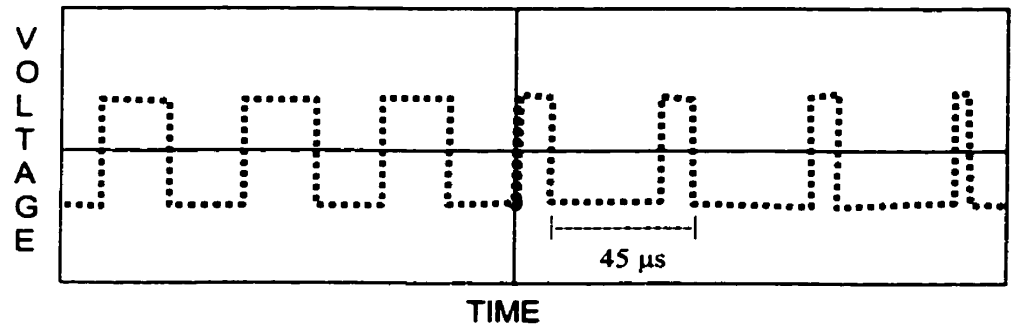

Figure 5.5. Diagram of Varying Duty Cycle.

As the duty cycle is changed, the average power given to the motor changes, thus modulating the motor output and corresponding grip force.

It was decided at that the slip system could interface directly with the VASI motor controller (see Appendix F). The point of interface within the controller circuit was looked at by Surry(1999) [2], and evaluated later on in the design process in this project when the system loop was closed. Using the VASI motor controller, the dead zone was no longer seen as a problem. The only consideration needed was that the slip signal should result in an output to the motor that would be sufficient to drive the motor past the dead-zone. This consideration was easy to implement electronically. The issue of hysteresis was also not seen as an issue. In fact, it was thought that it would help in conserving power by reducing the load on the motor, as originally intended in the mechanical design. Later on, when the completed prototype of the hand was made, as described in Section 5.7, the motor in fact did behave as expected and caused no problems.

5.2. PHASE AS A FUNCTION OF FREQUENCY

This experiment was set up by attaching a small flat speaker to the fingertips of the VASI 5-9 hand. A signal generator fed the speaker with a constant amplitude, variable frequency signal. The output from the sensors was seen on an oscilloscope. The amplitude and phase differences were measured for different values of frequencies. It was thought at first that the system would behave as a second order system, thus having one resonance frequency, which would produce a maximum amplitude, with zero phase shift at this frequency. Instead, the results proved to be surprising. As the frequency was raised, the phase difference between the signals from the two sensors changed. Eventually, the phase difference approached zero degrees, as expected. As the frequency was increased, the phase difference would increase until it reached a maximum of 180 degrees, and then decrease back down to zero degrees. This cycle occurred at regular frequency intervals. Following this cycle, the amplitudes, which varied slightly from each other, would increase and decrease periodically as a function of frequency, not just once as expected, but at regular, periodic frequency intervals. There was no one central resonance frequency, but many, which appeared at intervals of $3.0 \pm .5$ kHz. . The exact resonance frequency of one finger varied slightly from the other's.

Existing mathematical models of physical systems were searched to find one that corresponded most closely to this system's behaviour. The hand structure behaved as a carrier for sound waves. The resonance phenomenon appeared to resemble standing waves in a closed column, where the finger was the wave medium, the column.

This system is described by the equation:

$$\lambda = nl/2 \qquad \textit{Equation 2}$$

Where λ is the resonance wavelength, l is the column length, and n in a positive integer equal to or greater than 1. The equation derives from the fact that standing waves are only produced in a column whenever the wave fits exactly into the column, that is, when both ends of the column are at the zero points of the wave. See Figure 5.6.

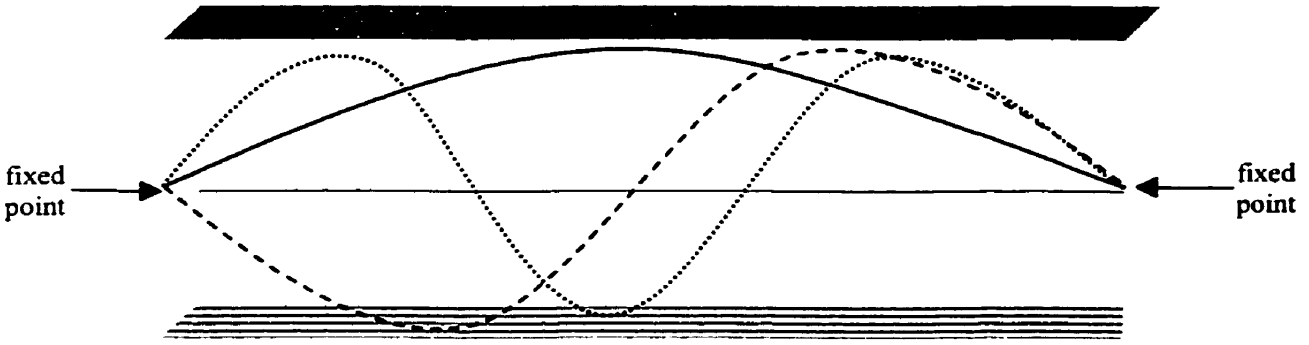

Figure 5.6. Standing Waves in a Closed Column. n=1,2,3.

Thus, each resonant peak corresponded to a half wavelength of the column's fundamental frequency, which must be in the order of 6 ± 1 kHz for VASI 5-9 finger. To verify this theory, the speed of wave propagation through the finger material was looked up, and the following equation was used to predict the length of the finger column:

$$c = \lambda f \qquad \textit{Equation 3}$$

Where c is the speed of sound or mechanical vibration through the medium, λ is the wavelength corresponding to the fundamental frequency, and f is the value of the fundamental frequency.

The length of the resonance tube was calculated using the equation for standing waves in a column for n=2. The material that the finger was made of is called Zytel ST801. It was originally thought that the waves resonate along the length of the finger, and thus the length of the finger would be equal to the primary resonance wavelength. However, the calculated wavelength did not correspond to the length of the tube, which is approximately 10 cm, but to its width, about 1 cm. This made sense, as the sensors were mounted on the front and back of the fingertip, not the top and bottom of the finger column. It was thought that the slight difference in length between the two fingers accounted for the slight difference in resonant frequency between the two fingers. These results led to the general approach taken in designing the noise reduction circuitry.

5.3. DESIGN APPROACH BASED ON SYSTEM CHARACTERISTICS

Once all three system parts were characterized, a general approach to circuit design was made based on the results of each part:

1. The relationship between amplitude and phase difference between two different sensor sites as a function of input frequency led to the standing wave model of the hand. Since the phase shift changed with frequency, it would be useful to look at only one frequency and use that as a signal. Since noise is broadband, a band-pass filter should be used to isolate just one output frequency. Then, phase shift and amplitude differences between the two sensors should be adjusted to produce zero ouput during

the noise condition. This would be done using phase shifter circuits and variable gain amplifiers. For this to work there must be a measurable phase or amplitude difference between responses to slip and noise, so that the slip signal would not be equal to the noise signal in the two sensors. Otherwise, adjusting the phase and amplitude differences to reduce noise would also reduce the slip signal output. Compliant fingertips may allow for mechanical separation of sensors to give a greater amplitude difference between the sensors. Sensor placement could lead to a phase difference between the two signals as well.

2. This part of the system characterization resulted in the analysis of the motor control circuitry to determine the proper interface point. After careful analysis of the control board circuit it was decided that if the output of the slip circuitry is conditioned properly, it could interface directly with the control board as an additional input. (See Appendix F for control board circuit)

3. The output stage of the system was characterized by measuring grip force vs. motor current. Although the overall response was nonlinear, no modifications needed to be made for proper control because the system operated within the linear response region. The amount of current used to drive the motor by the controller was above the dead-zone boundary. Since the slip system would only respond by closing the hand, it would not be affected by hysteresis, which is only seen when the hand is being opened.

The next step was to design, build, and test the actual circuits needed to implement the desired control and processing functions.

5.4. FIRST SETUP: SENSORS ON THE BACK ON EACH FINGER

The first complete setup of the sensors with the processing circuitry involved attaching two sensors to the back of each finger. The back was chosen to minimize interference that may occur on the sensors when they are pressed upon while the hand is gripping. First, the two sensors were connected directly to the IA, where the signals were subtracted. There was a noticeable output at the IA for both noise and slip, because the signals from the two sensors were not equal with respect to phase or amplitude.

Figure 5.7. Sensors on the Back of the Fingers.

The signal path was then taken from the sensors to a band-pass filter, a phase shifter, and then to the IA. The first thing that was examined was the effect of frequency on the output. Although the previous frequency analysis with a spectrum analyzer showed no distinct characteristics in the spectrum, the filters were swept through their range, and different combinations were tried. However, as anticipated, no noise reduction could be made based on frequency alone. Instead, both filters were tuned to a preset frequency. This helped to reduce EM noise, especially 60 Hz line noise. A centre frequency of 400 Hz was chosen, as it was a midpoint in the response range, and was used in previous slip

detection work [1,2]. (It also happens to be the resonance frequency in the human sensory neuron, the Pacinian corpuscle, which is the slip sensor in the human body. See Appendix A for more information on the physiological slip system). Also, since phase shift was a function of frequency, limiting the frequency range was thought to limit the phase distribution in the wide-band input, making it easier to manipulate the signals using the phase shifters. The phase shifter went after the filter, but before the IA.

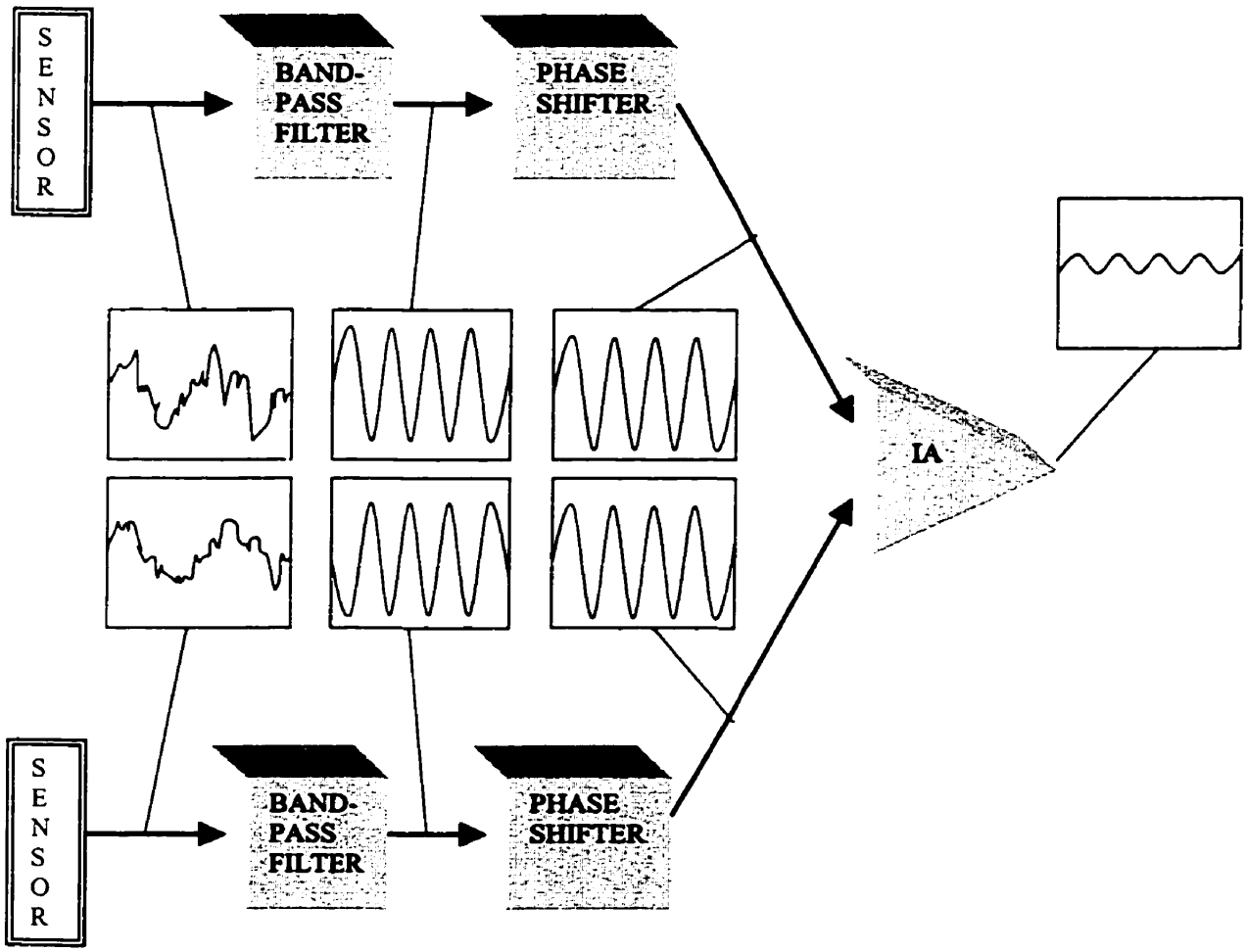

Figure 5.8. Experimental Setup and Oscilloscope Output at Points along the Signal Path.

The system was tuned using a 400 Hz signal from the speaker placed at the bottom of the hand, meant to simulate noise. The output of each signal was viewed on an oscilloscope, and the phase was manually adjusted using a trimmer, so that the phase difference came as close to zero as possible. It was possible to adjust the phase so that a slip signal was seen at the IA output, while the speaker input was seen as zero at the IA output. However, this did not prove to be the complete solution, because the slip signal itself was reduced as a result of the IA, and noise was still seen at the output of the IA when broad-band noise was used as an input by banging the hand. This was thought to be the result of two possible phenomena: The first hypothesis was that the filter was not specific enough, that is, the band-pass was not narrow enough, and a higher Q filter would be needed (higher Q means narrower and sharper band-pass). In later experiments (see Section 5.6), a higher Q filter was built to test this theory. However, the overall design was changed at that point, so this theory could not be fully investigated, and the results were inconclusive, although preliminary investigations indicated that this hypothesis was incorrect. The second hypothesis was that perhaps the sensors were too far apart, and that as the source of the noise signal moved, the phase and amplitude differences changed because one sensor appeared significantly closer to the signal source than the other. If this were true, it would violate the basic assumptions. So, to remedy this, a new design was sought.

5.5 SECOND CONFIGURATION: TWO SENSORS ON ONE FINGER

To bring the slip and noise sensors closer together physically, another pair of sensors was attached to the hand. Two more sensors were attached to each finger front, so that each finger now had a sensor on the front, and one on the back. The sensors were thus closer together and on the same finger, and any noise signal should appear more similar at the two sensors than previously. Being on opposite sides of the same finger, the column length in the standing wave model would be the same, and therefore the two sensors were expected to have a smaller and more constant phase difference.

Figure 5.9. Sensors on Front and Back of Fingers.

The first test used just the IA. The output showed both slip and noise, but less noise than before. However, it was then realized that even if the two signals were in phase, the sensors might be arranged so that after subtraction they are 180 degrees out of phase instead of 0 degrees. To verify this, one of the sensors was reversed in polarity relative to the other, so that its signal would effectively be inverted. This indeed gave a much smaller noise output, as expected. The same observations were made for the other finger in these two configurations. These observations further supported the standing wave model of the hand. Then, the combined parallel output from each finger was input into the IA. The IA output in this case included both noise and slip to the same extent as the first configuration. This is probably because the signals from the two different fingers, even if each finger has two sensors aligned in phase, result in a phase difference that

changed depending on the position of the noise source. A new setup was made to test this theory. The possibility was explored to have a satisfactory level of noise reduction with the two sensors on one finger. Three different circuit configurations were tried:

1. The two signals were run through a band-pass filter and phase shifter as before, and then to the IA. The phase was adjusted to minimize it during noise.
2. Same as in 1., expect two band-pass filters in series were used on each signal to increase the filter to fourth order in order to sharpen the filter response.
3. The signal was taken directly to the phase shifters, then to the IA, and the IA output was then band-pass filtered.

All three of these configurations suffered from the same drawback. While noise reduction was qualitatively good, certainly better than with the sensors on different fingers, the slip signal was also greatly reduced. This was counterproductive, because the goal of noise reduction was to increase the signal to noise ratio so that the slip signal could be easily distinguished from the noise, not to simply reduce the noise at the expense of the desired slip signal. The reduction in slip signal output was thought to be the result of the sensors being so close to each other. This resulted in too much "cross-talk". That is, if slip was present on the fingertip front and picked up by the front sensor, the back sensor would also sense a large slip signal. The same occurred with the noise signal. Even when the two sensors were on different fingers, cross-talk was observed. In order to separate the signals successfully, it became clear that the two sensors had to be mechanically isolated from each other in such a way that one would register slip more strongly than the other, while picking up the noise signal less than the other. This way,

when the gains are adjusted so that the noise signal is of equal magnitude at both sensors, there would be a measurable difference in the slip signal level between the two sensors. If the gain of the slip sensor is A, and the peak to peak voltages created by a noise signal at the slip sensor and noise sensor are x and y respectively, then the gain of the noise sensor should be adjusted to be equal to $A/(y/x)$ in order to maximize noise reduction when the signals from the slip and noise signals are differenced.

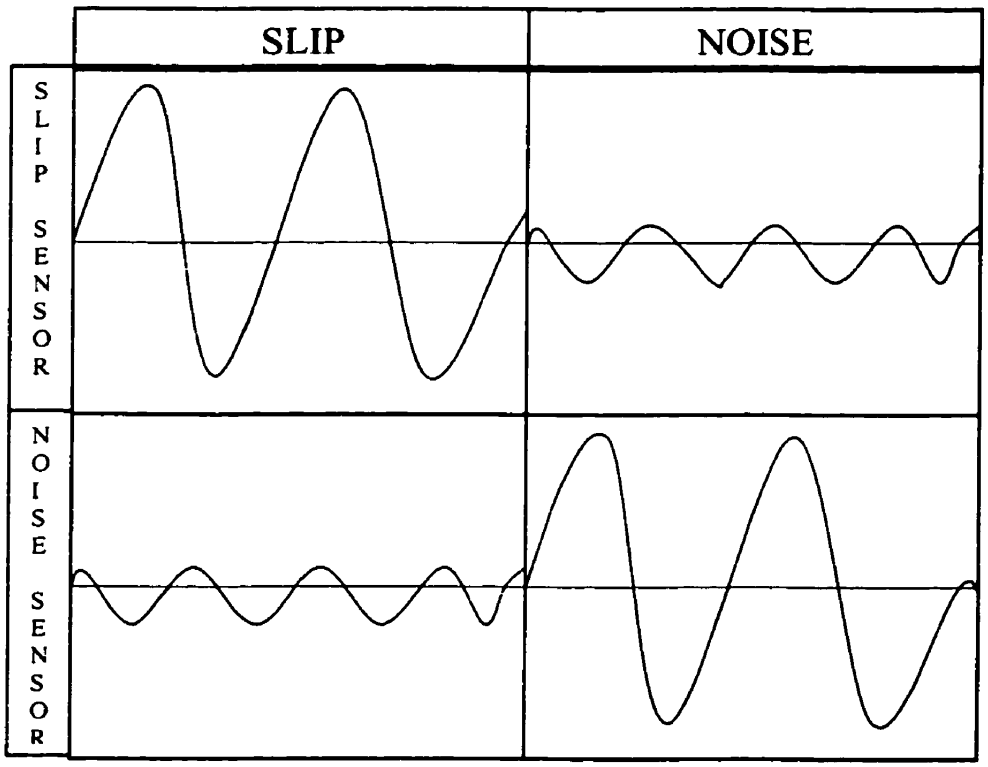

Figure 5.10. Separation of Slip and Noise signals.

It was decided that the best way to do this is by using a compliant fingertip as a mechanical vibration damper. Silicone is not a good conductor of sound, and a layer of silicone might work as a good sound insulator. It would have the added benefit of having a design that is compatible with compliant fingertips.

5.6. FINAL CONFIGURATION: THUMB WITH COMPLIANT FINGERTIP

This design was to have the slip sensor on top of a silicone fingertip on the thumb, and the other sensor attached to the back body of the thumb. Thus a slip signal would be registered at the slip sensor, but to get to the other sensor, which will be called the "noise sensor", the slip signal had to travel through the silicone, which dampens the signal, leaving a reduced level slip signal at the noise sensor. Conversely, a noise signal would be read with little attenuation at the noise sensor, since it is attached to the thumb body, but to reach the slip sensor, it would have to travel through the silicone insulation. Therefore, the noise signal would appear weaker at the slip sensor. Then, if the sensor gains were adjusted so that the output is equal for a common noise signal, the slip signal would appear much greater from the slip sensors than from the noise sensor, effectively increasing the signal to noise ratio.

Figure 5.11. Compliant Thumb with Sensors.

Another addition in this design was the use of a surface mount pre-amplifier located right at base of the thumb, so that the signal would be amplified without having to travel through any long wires. The purpose of this was to reduce EM interference from the 60 Hz line noise, which was sometimes a problem when the signals were highly amplified. The use of this pre-amplifier prevented EM noise pick-up along connection cables running the very high impedance, low level raw slip signal. By using a nearby pre-

amplifier, the signal level was increased, and the impedance was lowered, minimizing EM noise pickup from connecting wires.

Firstly, this new configuration was tested with the sensors going straight into the IA unprocessed to see if the silicone damping would be enough to eliminate noise altogether. While it did eliminate a lot of noise from the slip sensor, noise was still present. The next step was to run the signal through the band-pass filters, phase shifter and IA as before (see Figure 5.8), only this time, another component was added: a variable gain amplifier. This was added in order to finely adjust the gains of the two signals, so that their noise outputs would be equal. Again, the phase shifter was adjusted so that the phase shift was zero for a noise signal, which was provided by the speaker. Then the gains were adjusted to minimize the output. When minimized, there was still some noise output, but this time the signal-to-noise ratio (SNR) appeared higher than ever before. For the first time, it seemed as if the design might be good enough to try out in the complete system. Previously, most observations were made qualitatively, because the SNR was not high enough to warrant quantitative analysis (SNR worse than -6dB by observation). This time, the slip signal was clearly more than twice the amplitude of the noise signal, so the results were measured quantitatively. The output from both sensors was recorded straight from the band pass filter, then after the variable gain unit (after the gains were adjusted to reduce noise signal from a speaker source), and finally through the phase shifter circuit adjusted for zero phase shift. The overall SNR increased with each fine-tuning. Please see Table 3 for the results. Several oscilloscope readouts were recorded. The amplitude of each signal was simultaneously recorded using two oscilloscope

channels, the first for the slip sensor and the second for the noise sensor. The phase difference between the two signals was measured. Then, the oscilloscope output was changed to "difference" and the noise signal was subtracted from the slip signal. The amplitude of the differenced signal was recorded. A measure of noise reduction was calculated by dividing the amplitude of the differenced signal by the amplitude of the noise signal. The noise reduction was calculated in decibels.

	OUTPUT AFTER BAND-PASS FILTER	AFTER VARIABLE GAIN AMPLIFIER	AFTER PHASE SHIFTER
CHANNEL 1-SLIP SENSOR (mV)	15 ± 1	50 ± 2	50 ± 2
CHANNEL 2-NOISE SENSOR (mV)	22 ± 1	50 ± 2	50 ± 2
DIFFERENCE(mV)	10 ± 1	20 ± 2	1.5 ± .5
PHASE DIFFERENCE (°)	40 ± 10	40 ± 10	0 ± 5
NOISE REDUCTION Difference/Channel 2 (dB)	5	- 8	- 30

Table 3. Oscilloscope Output at three points in the Signal Processing Circuit for a Single Frequency Input

There was a total increase of 35dB of noise reduction gained by using the variable gain amplifier and the phase shifter, when both circuits were adjusted to minimize the output for noise.

Once again, even though the single frequency response was good, there was a response to broadband noise, as characterized by banging the hand. To further investigate this, the frequency of the speaker was swept and the results observed. As expected, the output was very low as the frequency drifted away from the centre frequency of the band-pass filter. However, what was unexpected was that very near the centre, the noise signal rose suddenly at two points before and after the centre frequency. This was accompanied by a corresponding phase shift. It was thought that this effect was causing noise to persist for a broadband stimulus, since the filter should clearly filter out most of the frequency response. If it was the frequencies near the centre that were causing trouble, than a filter with a very high Q might solve the problem.

Two more filters were built with a Q of 50, which gave a very narrow band-pass (see Appendix G). The experiment was repeated, but this did not remedy the solution, because the same phenomenon was observed, but on a narrower scale. At that point, investigation began to find out the source of the phase shift near the centre frequency. If it was the result of the filter characteristics, a new filter could be designed. If it was a characteristic of the mechanical system, then a new approach would be needed. The whole system was recontemplated, together with some new filter designs. This led to a new perspective of

the problem, which brought about a new and different solution to the phase shifting problem.

It became clear that the system could be designed to reduce noise based on differential amplitude characteristics of the two sensors, *or* phase difference characteristics, but both did not necessarily have to be used. One identifier or the other would do. Upon closer inspection, it became clear that the approach used thus far in the project was an attempt to actually separate the signals on the basis of amplitude. The issue of phase difference confused the whole matter because of the attempt to align the phases of the two signals so that their amplitudes would cancel out. The whole point of aligning the phases was to allow an amplitude difference measurement. Phase itself would never actually be used as a defining characteristic of the slip or noise signal, it was simply an extra artifact in the signal, and the previously mentioned designs tried to reduce its effects. (Note: D'Souza's [1] noise reduction approach actually used phase as the defining signal characteristic and not amplitude). If this was the case, then the easiest solution would have been to just measure the amplitude values of the two signals and take out phase from the signal altogether. This could be done electronically quite easily: First, the signal is rectified using a full wave bridge rectifier. This function takes the absolute value of the signal. Then, the varying AC component of the signal is filtered out, leaving only a DC value indicative of the average amplitude of the signal. In the next experiment, another circuit was used to do the same thing, only the signal was averaged using a peak detector circuit (see Appendix G). The two average signal outputs would then be subtracted in the IA. This would effectively take out the phase part of the signal, because the entire alternating

part of the signal has been removed. What is left is a signal that reflects the average signal amplitude level at each sensor site, which is really what was wanted all along. Using this method, quite satisfactory results were obtained.

This new circuit configuration was quantified with and without the noise cancellation system to check its effectiveness. The input was a speaker powered by a signal generator. The output voltage of the signal generator was varied. The speaker was set at three different places along the hand, to see the effect of signals from different sources. These sites were the bottom of the hand (as in the previous experiments), the finger tops, and the front (palmar region) of the thumb (where a slip signal would originate). See Figure 5.12. The results are shown in Figure 5.13.

Figure 5.12. Three locations of Speaker Input

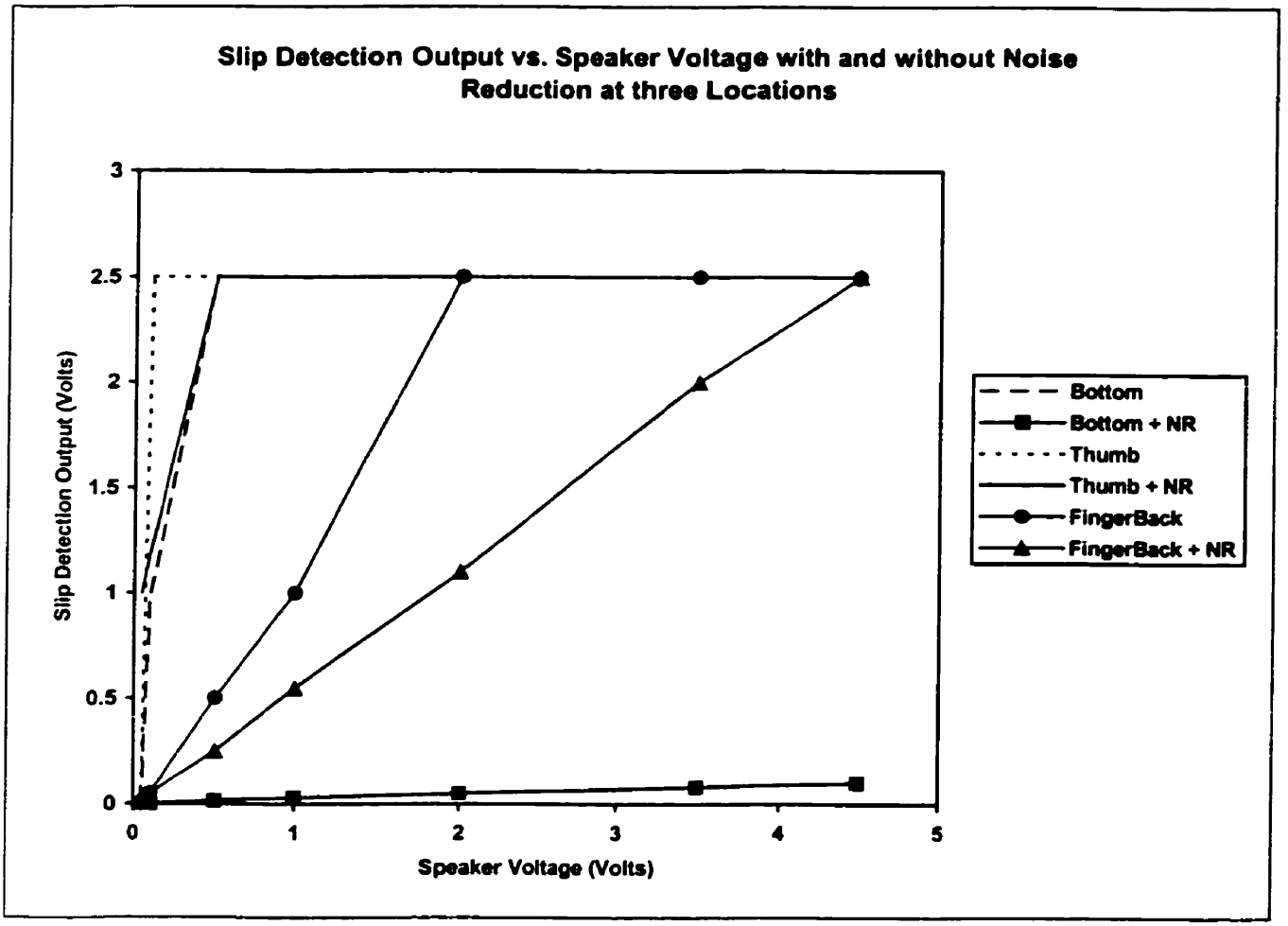

Figure 5.13. Slip Detection Output vs. Speaker Voltage with and without Noise Reduction at Three Locations.

Each result was be estimated as being approximately linear, and the gain was found as the slope of the line. The effect of the noise reduction system was seen as the ratio between the two gains with and without the noise reduction. The system was aligned with the signal source at the bottom of the hand, and noise was reduced by -35 dB. The noise reduction also reduced the slip signal level by –10 dB, as simulated by placing the speaker at the thumb location, where the slip sensors were located.

When the signal was at the fingertips, the noise reduction system was less effective than at the base of the hand, giving only –10dB of noise reduction. This illustrated the effect that the closer the signal source is to the slip sensors, the lower the SNR becomes, because the slip sensors picks up more noise signal. As such, a bang from beneath the hand, or from the table where the hand is sitting on may show little noise response, but a bang on the thumb or closer to it could produce a measurable output signal from the IA. However, these values are not the best estimate of the effectiveness of noise cancellation. The best indicator would be one in which the signal at the thumb is taken to represent the slip signal. If noise is then taken to come from the bottom, the SNR can be calculated with and without noise reduction, and the effect of the noise reduction system would then be clearer. The relation is seen in equation 4. In the equation, the desired signal is slip, which is represented by the word "*thumb*" to indicate the signal at the thumb where the slip sensor is located. The noise signal is represented by the signal at the bottom of the hand as "*bottom*", and *NR* stands for noise reduction. The ratio of the SNR without NR to the SNR with NR shows the effect of the noise cancellation system on the SNR.

$$\begin{aligned}
\textit{Effect of noise cancellation on SNR} &= \textit{(slip/noise) / (slip with NR/ noise with NR)} \\
&= \textit{(thumb/bottom) / (thumb with NR/ bottom with NR)} \\
&= \textit{(thumb/bottom)} \bullet \textit{(bottom with NR / thumb with NR)} \\
&= \textit{(thumb/thumb with NR)} \bullet \textit{(bottom with NR/ bottom)} \\
&= \textit{(35dB)} \bullet \textit{(-10db)} = \textit{(35 – 10) dB} \\
&= \textit{25 dB} \qquad \textbf{\textit{Equation 4}}
\end{aligned}$$

With the noise signal coming from the bottom, the noise cancellation circuit improved the SNR by 25 dB. Similarly, with the noise located at the finger backs, the same calculation shows that the SNR was improved by 0 dB, showing that as a noise signal comes closer to the slip sensors, the effect of the noise reduction system decreases. There was a 25 dB drop in SNR as the signal went from the bottom of the hand to the top of the fingers. This was thought to be due to an increase in the pickup of noise signal by the slip sensor as the noise signal got closer to the slip sensor.

The noise signal was reduced by 35 dB with both this processing circuit and the last one (See Table 3). The last circuit attempted to align the phase of the two signals such that the two signals canceled each other when their amplitudes were matched. It worked well for the test signal, but not for an actual banging of the hand. Earlier in the project, as seen in Section 5.4 and 5.5, it was thought that one reason for this could be that the phase relation between the two signals changed depending on the exact location of the noise source, so that the initial phase alignment was invalid in most noise situations. It was also thought in Section 5.4 that the phase difference changed as a function of frequency (possibly due to filter characteristics), so that a multi-frequency banging noise signal would only phase-align at one frequency, but a nearby frequency would still be out of phase, preventing cancellation. If these reasons for lack of noise cancellation during banging noise were correct, then taking the phase property entirely out of the signal would remedy the situation. This was done in the last circuit, but the problem persisted, indicating that these theories did not hold. However, the last experiment provided a clue into what might really be the cause of the inadequate noise cancellation. Note that the

noise signal in both circuits was reduced by 35 dB. This seems to indicate that the phase alignment circuit did indeed function effectively at removing the deleterious effect of phase on noise cancellation. However, when the signal was moved from the base of the hand, the noise cancellation was less effective, even though the phase property was not part of the signal anymore. It was also seen that the noise cancellation decreased as the noise signal came closer to the hand. In light of this information, the limitation of the noise cancellation system may be due to the limitation of using the amplitude of the two signals as the property that is compared. There seems to be a fundamental limitation to this method, because by pure reason one can see that if the noise signal source were at the slip sensor, the system would fail in recognizing the noise signal as such, and would see it as slip. The noise signal does not have to be 100% cancelled, since the output signal after noise reduction would only "on" if it was above a preset threshold value. This means that as the noise source came closer to the slip sensor, there would be a point where the threshold would be crossed, and the noise source would elicit a slip response. Of course, the less sensitive the slip sensor is to noise, the closer does the noise source have to come to the slip sensor to cross the threshold. An ideal slip sensor would be a unidirectional one, that is, a sensor that only responds to vibrations on its front surface but not its back surface. Using a compliant fingertip is one way of making the slip sensor less sensitive to noise. Another way to further insulate the slip sensor from mechanical noise could be to place a layer of acoustic insulation or a vacuum region beneath the compliant fingertip.

5.7. PERFORMANCE OF COMPLETED CLOSED LOOP SYSTEM

To verify the previous results, and to show that the hand did in fact work in its intended application in the final closed loop system, the rest of the circuits were built to complete the system. To complete the feedback loop, the slip signal had to be fed back to the control board. This proved to be a task initially, as the two circuit boards were not compatible. This was thought to be due to the power supplies. The main circuit board used a split power supply, while the control board did not. As such, a common ground could not be found. Instead, the system ran on two separate power supplies and was connected with an opto-isolator (see Appendix E). This device links electrical circuits with different grounds or power supplies using light as a connecting medium. One end of the opto-isolator was connected to the slip signal. The higher the signal, the brighter the LED inside it would shine. The LED shines on a phototransistor, which conducts current when light is present. The transistor output was then connected to the motor controller to complete the circuit. Thus when the slip signal was on, the motor received a current and was turned on, and the hand closed. The hand's sensitivity can be changed by adjusting the slip sensor's gain. If this is changed, care must then be taken to adjust the noise sensor's gain too, so that the noise signal is equal at both outputs and cancels out properly. The hand was set at medium sensitivity (the gain of the slip signal was halfway between its minimum and maximum). A rubbery object was placed in the hand, so that deformation of the object would indicate that the hand is gripping harder. At first, the hand's response was slow. It was found that the addition of the rubber glove improved the hand's response greatly. With the glove on, and some silicone grease under it, the

hand responded well to an object being pulled out. In fact, it was observed that the slip detection system was more sensitive with the glove *on*. This could have been due to the silicone grease increasing the contact surface with the object, together with the soft glove. This may have also been due to a greater coefficient of friction at the glove surface than at the sensor surface.

The system did not respond well if the object was pulled out too quickly. Banging from the table and near the bottom of the hand produced little or no response, but banging the hand near the middle or top produced a closing response. These responses were minimized by reducing the slip sensor's sensitivity, which was an acceptable solution because the fingertips were not desired to be too sensitive and over-responsive to slip. Overall, it was shown that the hand did respond well to slip in a controlled test situation with the glove on and with a compliant thumb, with some response to external noise. There were, however, several limitations that must be addressed so that further work on this project can deal with them.

5.8. LIMITATIONS

The most severe limitation was that the hand responded to noise from some external sources. There are several options that can be explored to reduce the effect of noise, such as using more noise sensors located at different points around the hand. These suggestions will be discussed in Section 6.3. Another limitation is the use of two power supplies. While this in not a major limitation in practice, some redesigning of the

circuit's voltage splitting section would be needed to allow operation with one power supply. Also, if the circuit's processing algorithm were to be made into a program and used with a microprocessor-based controller for the hand, then this would not be an issue anymore.

The circuit was built on a regular size circuit board. As such, it would not fit into an actual hand as of yet. It would have to be rebuilt on a small-scale printed circuit board using surface mount components to allow it to be housed within the actual hand. The current design would allow this to be easily done, since each component used was checked to make sure that a surface mount version is available.

6. CONCLUSIONS

6.1 CONCLUSIONS

A slip detection system for a child-sized myoelectric hand was built and tested. Different sensor locations were evaluated and different control circuits were tried. The best configuration was the one with the compliant fingertip, and a rectifying processor that converted the two signals into pure DC values, and then subtracted them. Careful trimming of individual sensor gains was needed for optimal operation. Final testing of the completed closed loop system showed a fully operating slip detection system with the cosmetic glove on, with some response to banging noise.

Most of the project objectives and goals were met. The original high-gear-ratio motor was tested and found to work with the slip detection system. PVDF piezoelectric polymer sensors were used, which made the system compatible with compliant fingertips. The closer match of acoustic impedance of the PVDF sensors to the PVC glove allowed the system to work properly with the cosmetic glove on. A very simply signal processing circuit was used that could easily be converted into a microprocessor routine if desired, or built using surface mount technology for installation inside the prosthetic. No complex digital signal processing, computer program, or neural network was needed to implement the system, unlike with other systems reported in the literature [1, 2, 9, 13]. The materials and methods used were simple, readily available, and inexpensive.

The slip detection system was brought closer to clinical implementation. The hypothesis was proven to be mostly correct: After the mechanical system was understood, it was manipulated, using filters, phase shifters, and compliant fingertips, which resulted in a more favorable output. These devices brought the system properties closer to the desired ones. The noise cancellation did not work in all the situations tested, only in limited situations, such as using a single frequency source, or banging from beneath the hand. As such, the performance of the hand was equivalent to the Otto Bock hand, which also responded to some noise. Compared to the slip detection system used by D'Souza [1] and Surry [2], this system was able to achieve several addition features, namely, compatibility with compliant fingertips and the cosmetic glove, and miniaturization. However, the stage of clinical testing was not reached.

6.2. CONTRIBUTIONS

The main contributions by the author came in the form of solutions to the problems encountered in previous research, through careful redesign of the slip detection system, thus bringing the research closer to clinical implementation. This research solved the following problems:

- The use of the original prosthetic hand motor was made possible by testing and characterizing the motor and ensuring its compatibility with the slip detection system. Previous work used an impractical, large, low gear-ratio motor.
- Compatibility with compliant fingertips was accomplished through the use of a piezoelectric polymer (PVDF) slip sensor. Previous work used an incompatible

piezoelectric ceramic sensor. It was shown that it *is* possible to implement a slip detection system with a prosthetic hand that has compliant fingertips.

- Miniaturization of the control circuitry was done using hardwired analogue circuits. Previous work used a desktop personal computer, which would be unusable in a clinical setting. It was demonstrated that a simple analogue controller could run a slip detection system, and that complex computational devices are not always necessary if the fundamental physical properties of the system are understood.
- Noise cancellation algorithms were developed based on principles of amplitude characterization. Previous work used noise cancellation based on phase properties, which is conceptually more difficult, and harder to implement practically. Noise cancellation was maximized by testing the effect of sensor placement on the hand, and by using different types of processing circuitry and techniques. The success of this was about equal to the only commercial available myoelectric hand slip detection system made by Otto Bock.
- Compatibility of the slip detection system with the cosmetic glove was achieved in the overall system. No reports of this accomplishment were previously published in the literature. However, the Otto Bock system does work with a glove on as well, although their glove material and design are significantly different from the ones used in this project.
- The slip detection system was tested and found to work satisfactorily with a child-sized myoelectric hand. The Otto Bock system is made only for adult sized hands.
- The slip detection system was found to function properly with compliant fingertips and a cosmetic glove in a child size myoelectric hand, a combined result previously

not found in any published papers or commercially available systems known to the author.

6.3 RECOMMENDATIONS FOR FURTHER WORK

The first recommendation is to improve the noise cancellation. It is thought that if additional noise sensors were used, instead of just one, then the hand would have less response to noise. This is because the noise signal would be a collection of all the noise signals around the body of the hand, making it less direction sensitive than it is now. Each noise sensor could have a separate gain, so that a "weighted" average of noise signal would be produced, to provide the most robust ratio between the noise sensors. Another improvement could be made by physically making the slip sensor less sensitive to noise signals. This could be done by placing a layer of acoustic insulation beneath the compliant fingertip on top of which the slip sensor lies. Since a vacuum is the best sound insulator, incorporating some sort of vacuum region beneath the slip sensor would make it less sensitive to noise.

The most robust noise cancellation system might be one that uses both amplitude and phase to determine whether slip has occurred. Amplitude characterization fails when the noise source is too close to the slip sensor. Using an additional circuit based on phase characterization would help in this situation. The system would only response to slip if *both* the amplitude and phase characterized circuits indicated slip at the same time.

In addition, the slip detection circuit and the motor controller should run on the same power supply. This could be done by redesigning the voltage splitting circuit that the amplifiers in the slip detection system use. However, this would not be a problem if the next recommendation was followed.

It may be desirable to implement the slip detection system using the MyoMicro technology that is already in use with the VASI hands. The processing algorithm could easily be written into a program and run digitally. After discussing this idea with staff at BMC's electronics department, it was learned that at the present time, the microprocessor used in the MyoMicro does not have enough memory to implement the system [27]. However, a new microprocessor, the PIC16F876, in the same line as the one currently used in the MyoMicro is now becoming available that has more memory, which could be used in the near future to implement the slip detection system [27]. This would reduce the system's physical space overhead to almost nothing, because most of the processing would take place in the microprocessor as software.

The response characteristics of the slip detection system should be tested, such as overshoot, oscillation and delay. This could be done in an experiment where a digital pinch force meter is used that has a digital output that can be transferred to a computer. This would allow a graph of pinch force vs. time to be generated. A known force function, such as a steadily increasing force, would pull the meter out of the hand. As the meter begins to slip, the grip force should increase, and this should be visible on the computer readout graph. When the grip is lost, the force would drop to zero. By using

different preset pulling functions and looking at the graph of grip force vs. time, the response time of the system could be measured. Having this quantity would allow for better assessment of the success of slip detection systems in the future.

Making the slip detection system part of the grasping algorithm described in Section 2.7 is highly recommended. An FSR could be used for the pressure sensors, and simple logic gates could implement the algorithm. This would likely increase the prosthetic hand's ease of use. However, this is not known for sure, so the next step needed would be clinical trials to see if there is any real advantage to the slip system and grasping algorithm.

Clinical testing of a prototype of the proposed design would be required. The experiment would consist of moving a variety of objects from place to place. The objects would be common household items of varying size, shape, weight and brittleness. These could include pencils, pens, eating utensils, stationery items like paperclips, eggs, milk cartons, books, and other items used in day-to-day activities. The factors that could be measured are the time it takes to complete the movement, and whether the object slips or breaks in the process. Stability of the object in grip would be tested by holding an object in the grip and subjecting it to a controlled hit of measurable force. These values would be compared to values obtained using an ordinary prosthesis as a control. Statistical analysis would then be performed to see if the system offers any significant advantage over ordinary myoelectric prosthetics.

The initial testing would be done on able-bodied adult subjects, since they would be easier to recruit and train than children with amputations. Note that anyone could use the system and be a test subject, since the myoelectric sensors can be placed on any muscles (the flexors and extensors of the forearm, for example), as can tactile feedback transmitters. The prosthesis could be hand-held or attached to the arm and then used to grasp objects and move them in a way similar to the real situation. After the initial testing, calibration, and debugging, clinical trials would be performed using children with amputations. The results of all of these tests would then be used to assess the success of the system and its clinical viability.

REFERENCES

1. D'Souza, W. *Tactile Sensing for Prosthetic Arms*. M.A.Sc. Thesis, Dept Of Mechanical Engineering, University of Toronto. 1996.

2. Surry, K. *Subconscious Control to Reduce Object Slip in Paediatric Myoelectric Hands*. M.A.Sc. Thesis. Dept of Mechanical and Industrial Engineering, University of Toronto. 1999

3. Joiner, J. *Guidelines for the Design of Electromechanical Hands and Incorporation of Compliant Fingertips*. M.A.Sc. Thesis, Dept Of Mechanical Engineering, University of Toronto. 1994.

4. Jacques, G E. *Powered Prosthetic Hand Function: Design Issues and Visual Feedback*. M.A.S.c. Thesis, Dept Of Mechanical Engineering. University of Toronto. 1994.

5. Eiss N S Jr., McCann B P. *Frictional Instabilities in Polymer-Polymer Sliding*. Tribology Transactions 36(4), pg. 686-692. 1993.

6. Lines, M E, and Glass, A M. *Principles and Applications of Ferroelectric Related Materials*. Clarendon Press, Oxford. 1977.

7. Kawai, H. *The Piezoelectricity of Poly(vinylidene Fluoride).* Jpn. J. Appl. Phys. Vol. 8, 975-976. 1969.

8. Bar-Cohen Y, et al. *Polymer Piezoelectric Transducers for Ultrasonic NDE.* NDTnet. Vol. 1 No. 9. Sept, 1996.

9. Petterson, P.E., Katz, J.A. *Design and Evaluation of a Sensory Feedback System that Provides Grasping Pressure in a Myoelectric Hand.* Journal of Rehabilitation Research and Development, 29(1). 1-8. 1992.

10. Scott, R.N. *Feedback in Myoelectric Prostheses.* Clinical Orthopaedics and Related Research, No. 256. 58-63. July 1990.

11. Meek S G, et al. *Extended Physiological Taction: Design and Evaluation of a Proportional Force Feedback System.* Journal of Rehabilitation Research and Development. Vol. 26 No. 3. 53-62. 1989.

12. http://www.novacaresabolich.com/newtech.html. *New Technology.* Nov 1999.

13. Canepa G, Petrigliano R, Campanella M, De Rossi D. *Detection of Incipient Object Slipage by Skin-Like Sensing and Neural Network Processing.* IEEE transcations on Systems, Man, and Cybernetics-Part B: Cybernetics. Vol. 28 No. 3.348-356. June 1998.

14. Tura A, et al. *Experimental Development of a Sensory Control System for an Upper Limb Myoelectric Prosthesis with Cosmetic Covering.* Journal of Rehabilitation Research and Development. Vol. 35 No. 1. 14-26. Jan 1998.

15. Hubbard S, Bush G, Kurtz I, Naumann S. *Myoelectric Prostheses for the Limb-Deficient Child.* Physical Medicine and Rehabilitation Clinics of North America. Vol. 2 No. 4. 847-866. Nov 1991.

16. http://www.mayohealth.org/mayo/9611/htm/artifici.htm. *Myoelectric Artificial Limbs.* Nov 1999.

17. http://www.mayohealth.org/mayo/9511/htm/artifica.htm. *Artificial Limbs.* Nov 1999.

18. Trembley M R, Cutkosky M R. *Estimating Friction Using Incipient Slip Sensing During a Manipulation Task.* Proc. IEEE International Conference on Robotics and Automation, 1993. Vol. 1. 429-432.

19. Kennedy, T. *Development of a Multi-Function Prosthetic Control System.* M.A.Sc. Thesis. Department of Mechanical Engineering. University of Toronto. 1998.

20. Dechev, N. *Development of Conformable Prosthetic Fingers.* M.A.Sc. Thesis. Department of Mechanical Engineering. University of Toronto. 1998.

21. Bloorview MacMillan Centre Annual Report, 1998-1999. *Variety Ability Systems Incorporated.* pg. 65.

22. Bloorview MacMillan Centre Annual Report, 1998-1999. pg. 2-36.

23. Variety Ability Systems Inc. *Small and Lightweight Electric Hands for Children.* 1996, Variety Ability Systems Inc., Toronto.

24. Otto Bock Product Information Brochure, 1998. *Automatic Grip Force with the SUVA-Sensor.* Can also be found at http://www.ottobock.com, Nov 1999.

25. http://www.msiusa.com . *Measurement Specialties, Inc.* Nov 1999.

26. AMP Sensors - Technical Manual. *Piezoelectric Film Properties.*

27. Personal communication. Electronics Dept at Bloorview MacMillan Centre.

28. Kyberd P J, Chappell P H. *The Southampton Hand: An Intelligent Myoelectric Prosthesis.* Journal of Rehabilitation Research and Development, Vol. 31, No.4. 326-334. 1994.

29. Personal communication. Hubbard S. Myoelectrics Dept at Bloorview MacMillan Centre.

APPENDIX A

A Systems Engineering Model of the Pacinian Corpuscle

This section is intended for readers with a biology background and little engineering and mathematics background. Its purpose is to explain some key basic concepts that are used in the body of the thesis using a biological example to illustrate the ideas. The example is an interesting parallel to the work in the thesis, because it is the physiological equivalent of the slip detection system. As such, this section might also be interesting to the engineer who wants to see how basic engineering concepts can be applied to a biological system. Mathematical modeling will be explained in general and applied to the case of the Pacinian Corpuscle.

The Pacinian corpuscle is a sensory neuron found in mammals. It detects mechanical vibrations in the outer layers of the skin. It is in the class of rapidly adapting mechanoreceptors; That is, it only responds to *changes* in pressure, like vibrations.

The physiological role of this type of sensor can be seen in the slip reflex mechanism. One place where Pacinian corpuscles are found and used to detect slip is the human fingertip [1]. When the fingertips hold an object, the pressure on them is constant. If the object begins to slip, due to the pull of gravity for example, friction between the object and the skin produces mechanical vibrations, which are detected by the Pacinian corpuscle. The result is a reflex muscle contraction to compensate for the grip until the vibrations stop. This reflex is also present in other parts of the mammalian body, and many experimenters use the cat's hind legs to measure this response [3]. The Pacinian corpuscle can be seen, in this regard, as a sensor, in the same way that a

microphone is a sensor. Both detect mechanical vibrations and convert them into electrical signals. Both have similar inputs and outputs, perhaps over different ranges, although their internal mechanisms are totally different. Is it possible to form a quantitative description of the similar aspects of these sensors while overlooking the differences in their internal mechanisms? It is, if they are seen as systems.

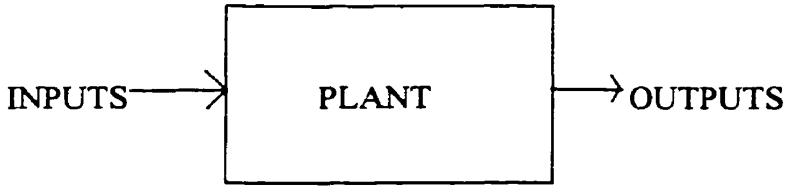

The part of the system that receives inputs and gives outputs, often called the plant, is like a black box; the inside is not always known. However, characteristics of the system can be determined by applying various inputs and looking at the outputs. How the system works internally is no longer a main concern. The trend of outputs for various inputs is the focus of systems analysis. If the output is known for a given input, then something crucial is known about the system. How the system works to do this is not important in this analysis, although knowing the input-output relationship may help to figure out the internal mechanism if we desire to do so later on. In this light, a system is anything that we can measure inputs and outputs from. A Pacinian corpuscle and a microphone are both systems. Both take mechanical vibrations as an input and produce electrical signals as an output. However, they have different internal mechanisms, yet perform the same function.

One method of analyzing the way in which the input is converted to output is by giving inputs over a wide range of frequencies and amplitudes and then measuring the output. This is called

frequency domain analysis, because the system's performance is seen over a spectrum of frequencies. Time domain analysis can also be used, in which the response of the system over time to a quick impulse is measured. However, to analyze the Pacinian corpuscle, only frequency domain analysis will be used.

The Pacinian corpuscle can be represented as a system. Let the input be a vibration, approximated by a sine wave. Thus, there are two input factors: the amplitude, A, and the frequency, ω. The Pacinian corpuscle then does whatever it does, and the output is measured as the number of action potentials per second, σ. This can be represented diagrammatically:

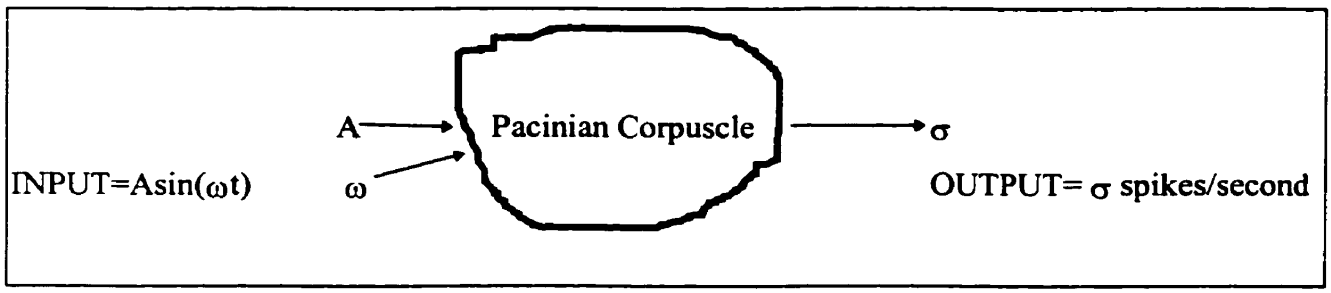

To learn about the properties of this system, an experiment was done by S.J Bolanowski and J.J. Zwislocki, which is found in the Journal of Neurophysiology, Volume 51 No.4, April 1984. Pacinian corpuscles were extracted and prepared. The input was mechanical sinusoidal vibrations produced by a speaker connected to a piece of glass that was in contact with the cell. The output was measured by an electrode counting the number of action potentials per second.
Now the input amplitude and frequency were changed to see the effect on the output. This was done by keeping the output constant at 1 spike/second, and then increasing the frequency

incrementally. The amplitude was then altered until the desired output was reached, and these values were noted.

The resulting graph looks like this:

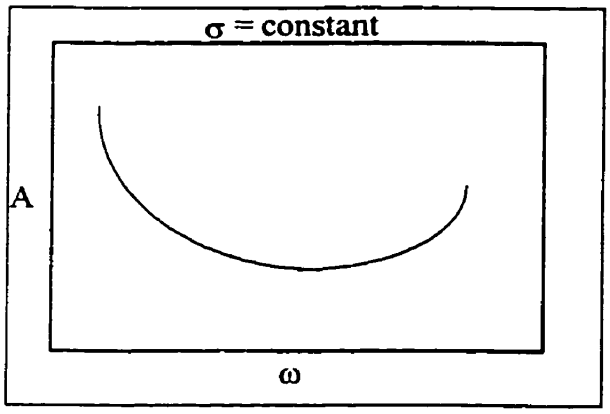

Modeling is a technique used to relate complicated unknown systems to systems that are familiar. To better understand how something works, it can be compared to something that is already understood. In studying mathematics, the behavior of mathematical functions and systems is analyzed in depth. If a physical system is compared to a mathematical system, the two might be similar enough that common characteristics will hold for both of them. The understanding of the familiar system can be applied to the unknown system. Since the realm of mathematics is infinite, this might be a formidable task. Still, in engineering, a perfect model is not required, only one that will work within specified parameters. The simplest model that accomplishes the task is chosen. A more complicated mathematical model might give higher accuracy, but the extra work of deriving this model is only justified if better accuracy is needed. The slip system and the Pacinian corpuscle can be modeled mathematically, and this model can be realized physically with the use of electronic devices. Many electronic devices are accurate reflections of

a mathematical model, and, as such, can be used to perform simple, and often complex, mathematical functions. In this way, the slip system and the Pacinian corpuscle system can be replicated, even though the internal mechanisms of the two systems may differ. Once a model is chosen, it can be tested for validity first by checking it against our experimental results, and then against others' experiments. If it still valid, it can be used to make predictions based on the new understanding of the system that the model has provided. Then further experiments can be performed to check whether the predictions were correct. If they were, then the model has succeeded in reflecting some of the true nature of the system. If not, then it is only accurate within limits that have been exposed. A model can be considered valid until it is proven otherwise. Ultimately, no model is perfect, because it is only an analogy, and not a true description of a system. As such, every model has limits. Still, its use is valuable in engineering. If its limits are kept in mind, a model can be used to perform necessary calculations, and often the required performance specifications are within the limits of the model. Although they might not be perfect, they will be close enough for the given needs if the limits are not exceeded. Since many simple models are linear, their limit is reached at the point where they become nonlinear.

The input-output relationship is called linear if the following condition holds:

For $y=f(x)$, if $y_1 = f(x_1)$ and $y_2 = f(x_2)$

then $y_3 = y_1+y_2 = f(x_1+x_2)$

All real physical systems are in fact nonlinear. However, many of these are linear over a certain range, or can be approximated by linear functions. If a simple linear function describes a system to our desired degree of accuracy, then this model is sufficient from an engineering point of view. Even though a nonlinear model might be more realistic in describing a system, it is not necessarily needed in practical application if a simpler linear model does the job. Linear systems are much easier to analyze than nonlinear ones. In fact, classic systems theory deals mainly with linear time invariant systems. Time invariance means that the system behaves the same way, independent of time. That is, if it is f(x)=10x at one point in time, it will be f(x)=10x at any other point in time. Real physical systems are also causal. That is, there are only outputs in direct response to inputs. This means that the output is zero for time less than zero.

The following is an example of a nonlinear system that can be described as linear over certain ranges. A linear model can be used to describe the system between *{-B,B}*. However, outside this range, the model will not hold anymore. Still, if it is known that the system will always be inside this range for all the given needs, the model can be used. If, in the future, specifications change and the system needs to operate over a wider range, a new model will have to be made. In some cases, like in the example, it can be a piecewise linear model.

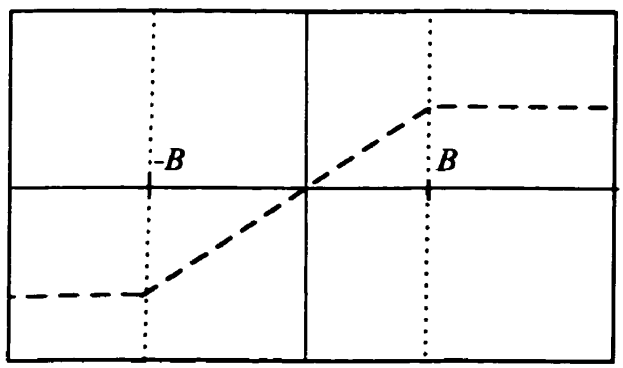

Assume that the Pacinian corpuscle system is actually comprised of two systems, an electrical system and a mechanical system. This is justified, since the morphology of the cell, hence its mechanical properties, is known to be responsible in some way for its response to vibration characteristics, and since neurons are known to function based on changes in electrochemical gradients [2]. Thus the cell can be modeled using the known models for mechanical and electrical systems. Now all that is needed is a mathematical model or a circuit diagram that adequately describes the experimental results.

The first to be determined is how many components the circuit will have, and then their relative orientation. By looking at the graph, it is at least a second order differential equation. A zero order equation would have no change as a function of change in time (dt). Its slope (first derivative) will be zero. Therefore, it would be independent of frequency, and the graph would be a horizontal line. If it was a first order differential equation, it would change with respect to a change in time. That is, its slope will be a constant, so the slope of the slope (the second derivative) will be zero. Thus, it would be a straight line. Now, a second order equation will change twice with respect to a change in time, so its slope will change with respect to time, and the second derivative will be constant. It is clear from the graph of the experimental results, that the slope is not zero and the slope is not constant. We cannot tell if the slope of the slope is constant, so let us assume it is for a first approximation. If this approximation is sufficient in describing the results, we need not go further into higher order differential equations, which are harder to solve.

When two dynamic electrical components are used, it is possible to produce differential equations up to a second order to describe the system. Since the output will change in proportion to changes in the input, to fully describe the system we need to look at it when the input is changing at different rates. If the input is a sine wave, $A\sin(\omega t)$, where ω is the frequency and A is the amplitude, the output, $B\sin(\omega t + \phi)$ will have the same frequency since the system is linear and time invariant, but its amplitude, B, may be different and may vary as a function of ω. It will also have a phase difference,ϕ, also a function of ω. The gain of the system is the output/input. A Bode plot is a graph of the gain of the system as a function of frequency, usually on a logarithmic scale. It is also accompanied with a graph of the phase difference as a function of frequency. These graphs can be determined analytically if the notation is changed to polar co-ordinates, which will allow the frequency response of the individual elements to be seen, as well as systems made up of a combination of them.

Intuitively, if a capacitor is examined, the current is proportional to the rate of change in voltage. This means that the faster the voltage changes, the larger will be the current. If the voltage is a sinusoid, the current will be proportional to the frequency of the sinusoid. This result can be stated mathematically. Let the voltage, $V(t) = V\cos(\omega t + \phi)$.

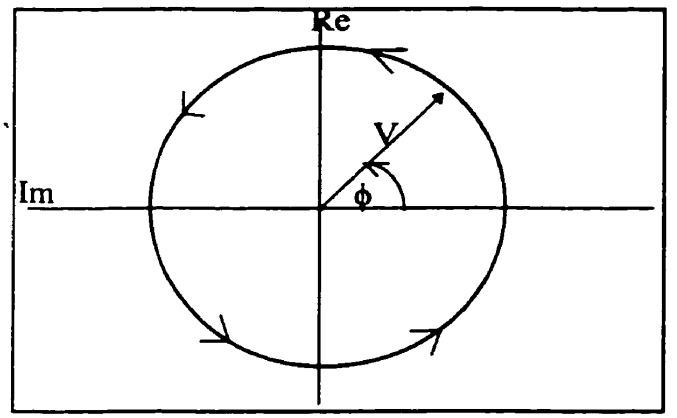

Its polar form is $V\angle\phi$, rotating at the frequency ω. This can also be represented in the complex plane using Euler's formula: $e^{j\omega t} = \cos(\omega t) + j\sin(\omega t)$, where $j = \sqrt{-1}$. Here, a unit vector will rotate in a circle around the origin in the complex plane at a frequency ω. This can be represented on any co-ordinate system, but using the real and imaginary axis allows us to use identities of complex numbers to simplify calculations. Now we can represent the input sinusoid as $V(t) = Ve^{j\omega t}$. Note that the phase angle has been omitted for simplicity. The phase has very significant importance, but for now, let us look only at the frequency dependence of the amplitude of V(t).

For a capacitor, $I(t) = C \cdot dV(t)/dt = C \cdot d(Ve^{j\omega t})/dt = C \cdot j\omega \cdot Ve^{j\omega t} = j\omega C \cdot V(t)$

Thus the mathematical relationship of V and I as a function of frequency is seen.

Similarly, the relationship for an inductor is found, $V(t) = j\omega L \cdot I(t)$. The resistor's current voltage relationship is independent of frequency. The impedance, Z, is a representation of the current voltage relationship, where $Z = V/I$. As such, the impedance of a capacitor is $Z = 1/j\omega C$, for an inductor it is $Z = j\omega L$, and for a resistor it is $Z = R$. This notation can be used to solve the input output function for systems with all three components in them, as a function of frequency.

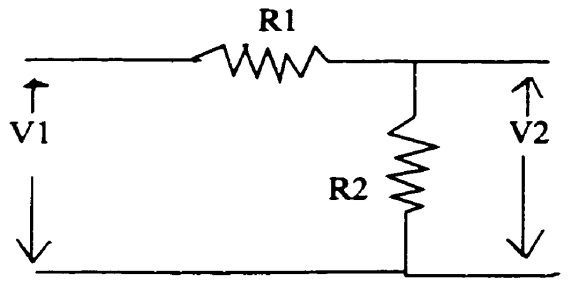

For the above system, where V1 is the input and V2 is the output, the gain, G=V2/V1 is given by V2=V1(R2/R1 + R2), or G = R2/R1 + R2.

Now substitute the resistors with impedances to form a frequency dependent gain. First let R2 be a capacitor and an inductor in series:

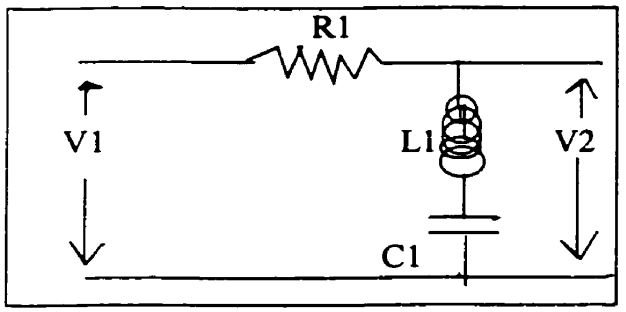

Now $G = Z2/ Z1+ Z2$ where $Z1 = R1$ and

$Z2 = Z(L1) + Z(C1) = j\omega L + 1/j\omega C$

So $G = (j\omega L + 1/j\omega C)/ (R + j\omega L + 1/j\omega C)$.

When $\omega = 0$, G=1. When $\omega = \infty$, G=1. In between, the gain drops to zero and rises back to one. To find the frequency at which the gain is zero, solve for ω at G=0.

$$0 = j\omega L + 1 / j\omega C$$
$$\omega = 1 / \sqrt{LC}$$

This is called the resonance frequency.

The graph of the gain versus frequency is shaped like this:

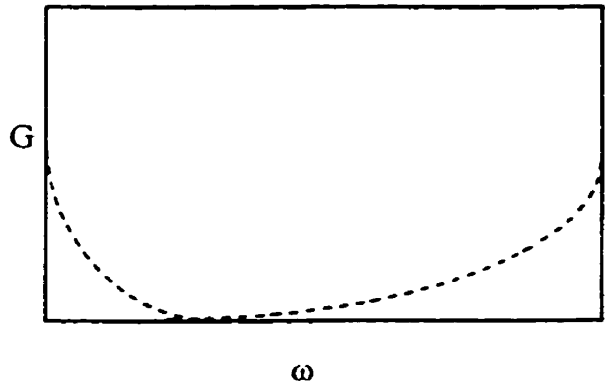

Another type of frequency relation can be seen when the capacitor and inductor are place in parallel:

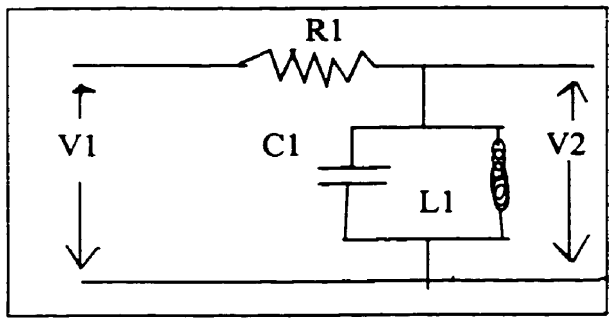

In this case, $Z2 = 1/(1/j\omega L + j\omega C)$.

So $G = Z2/Z1+Z2 =$

$1/(1/j\omega L + j\omega C)// R + 1/(1/j\omega L + j\omega C)$

For this system, $G=0$ when $\omega=0$ and $\omega = \infty$.

$G=1$ when $\omega = 1 / \sqrt{LC}$, the resonance frequency.

The graph of gain versus frequency looks like this:

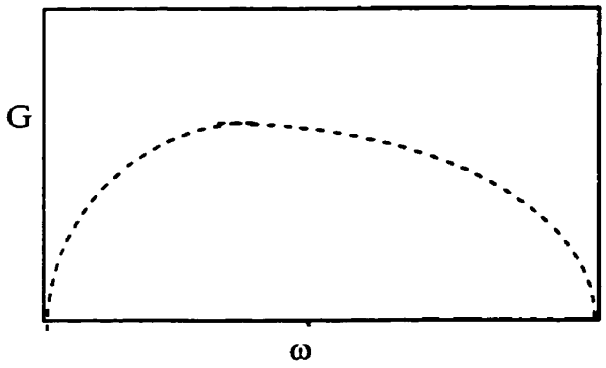

Now that we have looked at some circuits described by second order equations, let us see if we can match one of them to our experimental results and use it as a model for our system.

First, we need to convert the experimental results, plotted as amplitude versus frequency, so as to obtain a graph of gain versus frequency. The gain for our system is $G = A/\sigma$, the output divided by the input, which will vary with frequency. If we divide the amplitude axis by σ, which is constant, the graph will have the same shape as the original, though scaled differently. Then, if we take the reciprocal on that axis, the result is σ/A, the gain, as desired. The graph will be inverted: small values will become large, and large values will become small.

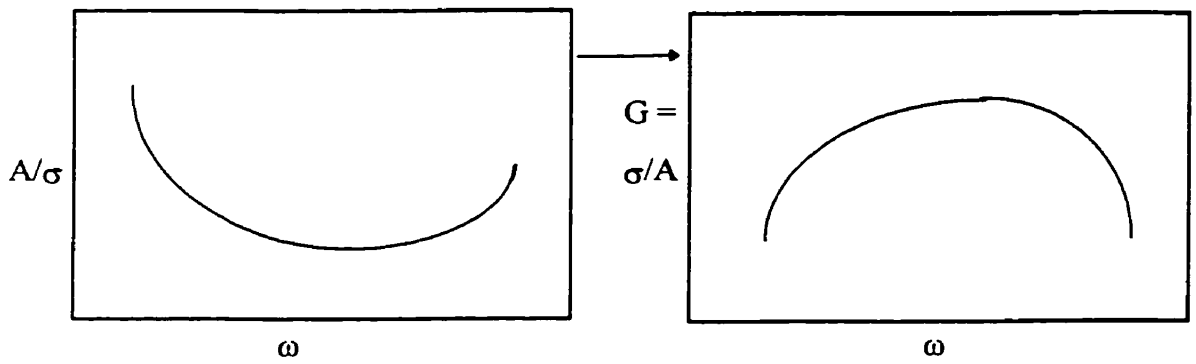

The graph of gain versus frequency is similar to the last circuit described, with the capacitor and inductor in parallel. For the experiment, the resonance frequency was about 400 Hz. Using the model, this means that $1/LC=(400)^2$, or $C=1/(160000 \cdot L)$. The input amplitude at resonance was about 3 mm. This gave an output of 1 impulse/second. The gain at resonance for our system is one. To account for this, we can add a component to the system, a gain of

(1000/3) impulse/mm·second. We know that the gain is zero at zero frequency, since a vibration is needed to produced an output. We can't measure infinite frequency, but the gain seems to decrease as frequency is increased. Using this analysis, we can write our model as such:

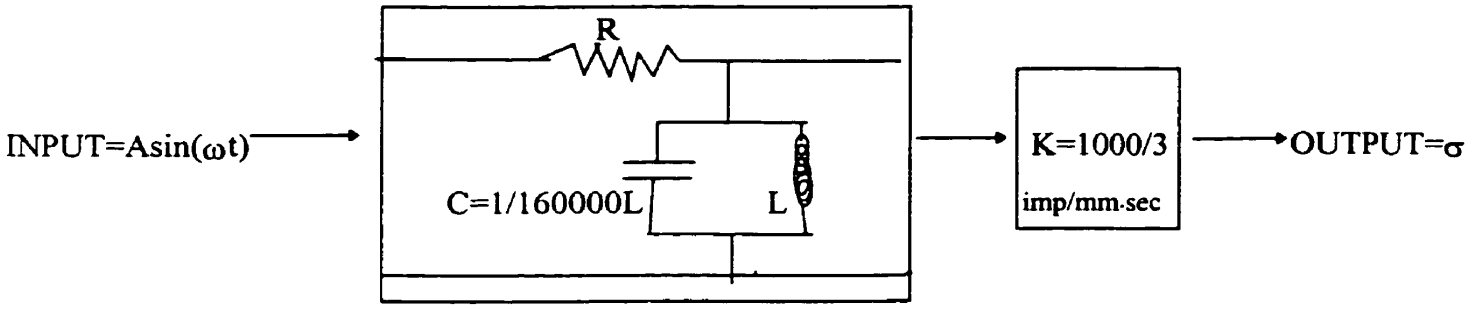

We can simulate our model by building an electronic circuit, and use it to predict values outside of the original experimental range. Then we can go and do another experiment to see how well the model works. If our model is able to predict these values, then we know it is a good reflection of the real system.

REFERENCES

1. Srivnivasan M A, Whithouse J M, LaMotte R H. *Tactile Detection of Slip: Surface Microgeometry and Peripheral Codes.* J Neurophysiology. 63(6). Jun 1990. 1323-1332.

2. Johansson R S, Westling G. *Signals in Tactile Afferents from the Fingers Eliciting Adaptive Motor Responses During Precision Grip.* Exp Brain Res. 66. 1987. 141-154.

3. Haugland M K, Hoffer J A, Thomas S. *Skin Contact Force Information in Senory Nerve Signals Recorded by Implanted Cuff Electrodes.* IEEE Trans Rehab Eng. 2(1). 18-28.

APPENDIX B: PVDF Properties

Symbol	Parameter		PVDF	Copolymer	Units
t	Thickness		9, 28, 52, 110	Various	μm (micron, 10^{-6})
d_{31}	Piezo Strain Constant		23	11	10^{-12} $\frac{m/m}{V/m}$ or $\frac{C/m^2}{N/m^2}$
d_{33}			-33	-38	
g_{31}	Piezo Stress Constant		216	162	10^{-3} $\frac{V/m}{N/m^2}$ or $\frac{m/m}{C/m^2}$
g_{33}			-330	-542	
k_{31}	Electromechanical Coupling Factor		12%	20%	
k_t			14%	25-29%	
C	Capacitance		380 for 28 μm	68 for 100 μm	pF/cm^2 @ 1kHz
Y	Young's Modulus		2-4	3-5	10^9 N/m^2
V_0	Speed of Sound	stretch:	1.5	2.3	10^3 m/s
		thickness:	2.2	2.4	
p	Pyroelectric Coefficient		30	40	10^{-6} C/m^2 °K
ε	Permittivity		106-113	65-75	10^{-12} F/m
$\varepsilon/\varepsilon_o$	Relative Permittivity		12-13	7-8	
ρ_m	Mass Density		1.78	1.82	10^3kg/m
ρ_e	Volume Resistivity		>10^{13}	>10^{14}	Ohm meters
R	Surface Metallization Resistivity		2.0	2.0	Ohms/square for CuN
R			0.1	0.1	Ohms/square for Ag Ink
$\tan\delta_e$	Loss Tangent		0.02	0.015	@ 1kHz
	Yield Strength		45-55	20-30	10^6 N/m^2 (stretch axis)
	Temperature Range		-40 to 80	-40 to 115...145	°C
	Water Absorption		<0.02	<0.02	% H_2O
	Maximum Operating Voltage		750 (30)	750 (30)	*V/mil* (*V*/μm), DC, @25°C
	Breakdown Voltage		2000 (80)	2000 (80)	*V/mil* (*V*/μm), DC, @25°C

APPENDIX C: OPERATIONAL AMPLIFIER SPECIFICATIONS

National Semiconductor

November 1994

LMC6062 Precision CMOS Dual Micropower Operational Amplifier

General Description

The LMC6062 is a precision dual low offset voltage micropower operational amplifier, capable of precision single supply operation. Performance characteristics include ultra low input bias current, high voltage gain, rail-to-rail output swing, and an input common mode voltage range that includes ground. These features, plus its low power consumption, make the LMC6062 ideally suited for battery powered applications.

Other applications using the LMC6062 include precision full-wave rectifiers, integrators, references, sample-and-hold circuits, and true instrumentation amplifiers.

This device is built with National's advanced double-Poly Silicon-Gate CMOS process.

For designs that require higher speed, see the LMC6082 precision dual operational amplifier.

PATENT PENDING

Features (Typical Unless Otherwise Noted)

- Low offset voltage 100 μV
- Ultra low supply current 10 μA/Amplifier
- Operates from 4.5V to 15V single supply
- Ultra low input bias current 10 fA
- Output swing within 10 mV of supply rail, 100k load
- Input common-mode range includes V⁻
- High voltage gain 140 dB
- Improved latchup immunity

Applications

- Instrumentation amplifier
- Photodiode and infrared detector preamplifier
- Transducer amplifiers
- Hand-held analytic instruments
- Medical instrumentation
- D/A converter
- Charge amplifier for piezoelectric transducers

Connection Diagram

S.T.M.E. for TLC272

8-Pin DIP/SO

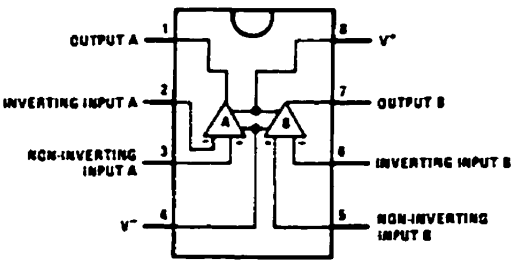

TL/H/11208–1

Top View

Ordering Information

Package	Temperature Range		NSC Drawing	Transport Media
	Military −55°C to +125°C	Industrial −40°C to +85°C		
8-Pin Molded DIP	LMC6062AMN	LMC6062AIN LMC6062IN	N08E	Rail
8-Pin Small Outline		LMC6062AIM LMC6062IM	M08A	Rail Tape and Reel
8-Pin Ceramic DIP	LMC6062AMJ/883		J08A	Rail

APPENDIX D: INSTRUMENTATION AMPLIFIER SPECIFICATIONS

LINEAR TECHNOLOGY

LT1101

Precision, Micropower, Single Supply Instrumentation Amplifier (Fixed Gain =10 or 100)

FEATURES

- Gain Error — 0.04% Max
- Gain Non-Linearity — 0.0008% (8ppm) Max
- Gain Drift — 4ppm/°C Max
- Supply Current — 105μA Max
- Offset Voltage — 160μV Max
- Offset Voltage Drift — 0.4μV/°C Typ
- Offset Current — 600pA Max
- CMRR, G = 100 — 100dB Min
- 0.1Hz to 10Hz Noise — 0.9μVp-p Typ, 2.3pAp-p Typ
- Gain Bandwidth Product — 250kHz Min
- Single or Dual Supply Operation
- Surface Mount Package Available

APPLICATIONS

- Differential Signal Amplification in Presence of Common-Mode Voltage
- Micropower Bridge Transducer Amplifier
  - Thermocouples
  - Strain Gauges
  - Thermistors
- Differential Voltage to Current Converter
- Transformer Coupled Amplifier
- 4mA-20mA Bridge Transmitter

DESCRIPTION

The LT1101 establishes the following milestones:
(1) It is the first micropower instrumentation amplifier,
(2) It is the first single supply instrumentation amplifier,
(3) It is the first instrumentation amplifier to feature fixed gains of 10 and/or 100 in low cost, space-saving 8-lead packages.

The LT1101 is completely self-contained: no external gain setting resistor is required. The LT1101 combines its micropower operation (75μA supply current) with a gain error of 0.008%, gain linearity of 3ppm, gain drift of 1ppm/°C. The output is guaranteed to drive a 2k load to ±10V with excellent gain accuracy.

Other precision specifications are also outstanding: 50μV input offset voltage, 130pA input offset current, and low drift (0.4μV/°C and 0.7pA/°C). In addition, unlike other instrumentation amplifiers, there is no output offset voltage contribution to total error.

A full set of specifications are provided with ±15V dual supplies and for single 5V supply operation. The LT1101 can be operated from a single lithium cell or two Ni-Cad batteries. Battery voltage can drop as low as 1.8V, yet the LT1101 still maintains its gain accuracy. In single supply applications, both input and output voltages swing to within a few millivolts of ground. The output sinks current while swinging to ground — no external, power consuming pull down resistors are needed.

BLOCK DIAGRAM

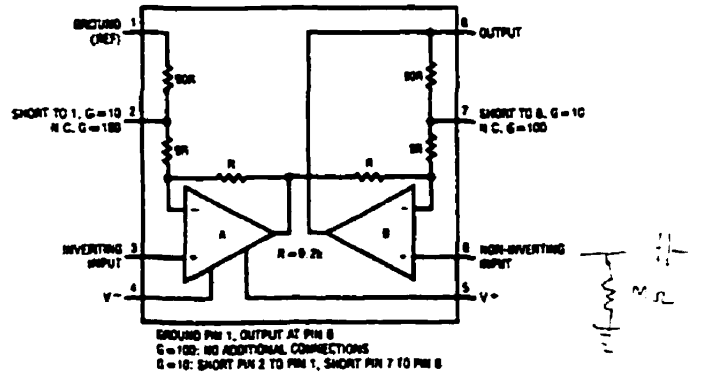

Gain Error Distribution

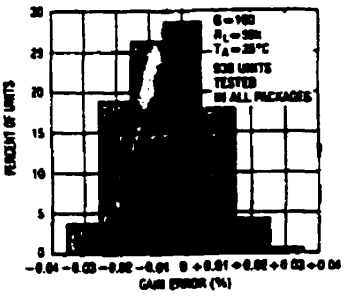

APPENDIX E: OPTO-ISOLATOR SPECIFICATIONS

MOTOROLA

4N25, 4N25A
4N26
4N27
4N28

NPN PHOTOTRANSISTOR AND PN INFRARED EMITTING DIODE

...Gallium Arsenide LED optically coupled to a Silicon Photo Transistor designed for applications requiring electrical isolation, high-current transfer ratios, small package size and low cost; such as interfacing and coupling systems, phase and feedback controls, solid-state relays and general-purpose switching circuits.

- High Isolation Voltage — V_{ISO} = 7500 V (Min)
- High Collector Output Current @ I_F = 10 mA — I_C = 5.0 mA (Typ) — 4N25,A,4N26; 2.0 mA (Typ) — 4N27,4N28
- Economical, Compact, Dual-In-Line Package
- Excellent Frequency Response — 300 kHz (Typ)
- Fast Switching Times @ I_C = 10 mA t_{on} = 0.87 µs (Typ) — 4N25,A,4N26; 2.1 µs (Typ) — 4N27,4N28 t_{off} = 11 µs (Typ) — 4N25,A,4N26; 5.0 µs (Typ) — 4N27,4N28
- 4N25A is UL Recognized File Number E54915

OPTO COUPLER/ISOLATOR

TRANSISTOR OUTPUT

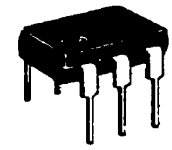

*MAXIMUM RATINGS (T_A = 25°C unless otherwise noted).

Rating	Symbol	Value	Unit
INFRARED-EMITTING DIODE MAXIMUM RATINGS			
Reverse Voltage	V_R	3.0	Volts
Forward Current — Continuous	I_F	80	mA
Forward Current — Peak (Pulse Width = 300 µs, 2.0% Duty Cycle)	I_F	3.0	Amp
Total Power Dissipation @ T_A = 25°C (Negligible Power in Transistor)	P_D	150	mW
Derate above 25°C		2.0	mW/°C
PHOTOTRANSISTOR MAXIMUM RATINGS			
Collector-Emitter Voltage	V_{CEO}	30	Volts
Emitter-Collector Voltage	V_{ECO}	7.0	Volts
Collector-Base Voltage	V_{CBO}	70	Volts
Total Device Dissipation @ T_A = 25°C (Negligible Power in Diode)	P_D	150	mW
Derate above 25°C		2.0	mW/°C
TOTAL DEVICE RATINGS			
Total Device Dissipation @ T_A = 25°C	P_D	250	mW
Equal Power Dissipation in Each Element			
Derate above 25°C		3.3	mW/°C
Junction Temperature Range	T_J	-55 to +100	°C
Storage Temperature Range	T_{stg}	-55 to +150	°C
Soldering Temperature (10 s)		260	°C

*Indicates JEDEC Registered Data.

FIGURE 1 — MAXIMUM POWER DISSIPATION

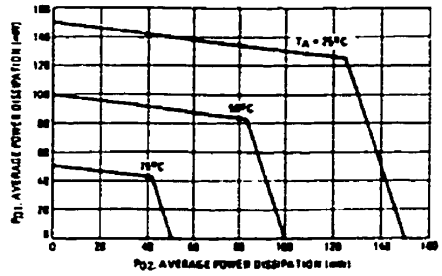

Figure 1 is based upon using limit values in the equation.

$T_{J1} - T_A = R_{\theta JA}(P_{D1} + K_\theta P_{D2})$

where:

T_{J1} Junction Temperature (100°C)
T_A Ambient Temperature
$R_{\theta JA}$ Junction to Ambient Thermal Resistance (500°C/W)
P_{D1} Power Dissipation in One Chip
P_{D2} Power Dissipation in Other Chip
K_θ Thermal Coupling Coefficient (20%)

Example

With P_{D1} = 90 mW in the LED @ T_A = 50°C, the transistor P_D (P_{D2}) must be less than 90 mW.

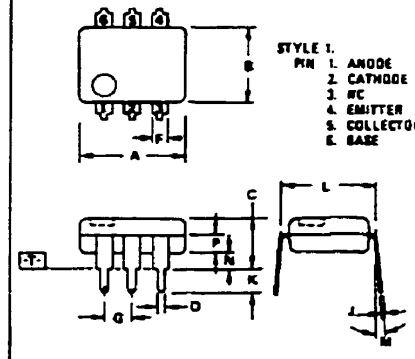

NOTES:
1. DIMENSIONS A AND B ARE DATUMS.
2. -T- IS SEATING PLANE.
3. POSITIONAL TOLERANCES FOR LEADS
4. DIMENSION L TO CENTER OF LEADS WHEN FORMED PARALLEL.
5. DIMENSIONING AND TOLERANCING PER ANSI Y14.5, 1973.

DIM	MILLIMETERS MIN	MILLIMETERS MAX	INCHES MIN	INCHES MAX
A	6.13	6.60	0.220	0.260
B	6.10	6.60	0.240	0.260
C	2.92	3.68	0.115	0.200
D	0.41	0.51	0.016	0.020
F	1.02	1.78	0.040	0.070
G	2.54 BSC		0.100 BSC	
J	0.20	0.30	0.008	0.012
K	2.54	3.81	0.100	0.150
L	7.62 BSC		0.300 BSC	
M	0°	15°	0°	15°
N	0.38	2.54	0.015	0.100
P	1.27	2.03	0.050	0.080

CASE 730A-01

APPENDIX F: VASI 5-9 MOTOR CONTROL CIRCUIT

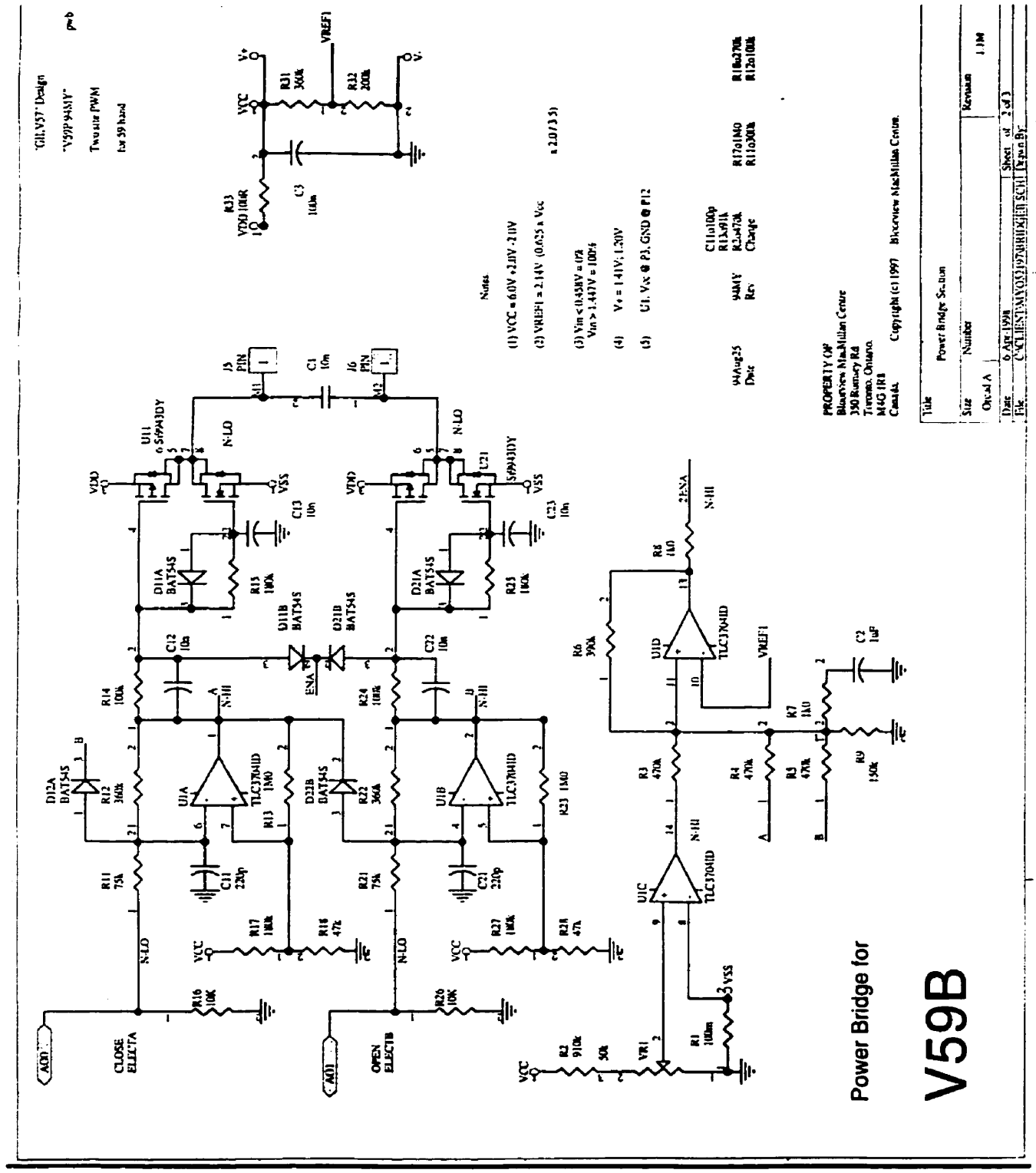

APPENDIX G: CIRCUIT BUILDING BLOCKS

High Q filter

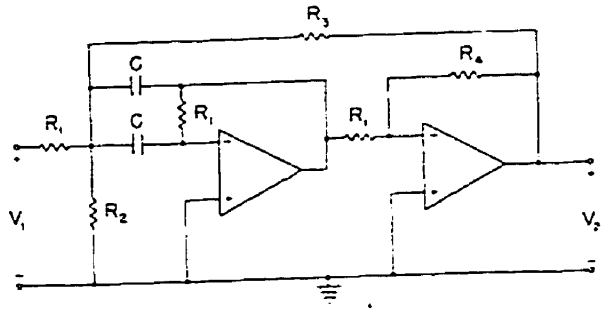

Band-pass filter

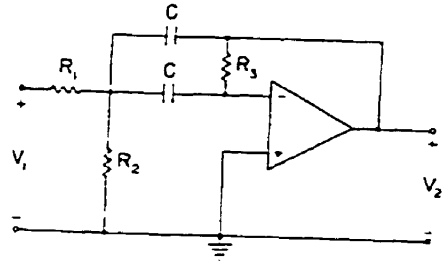

PEAK DETECTOR

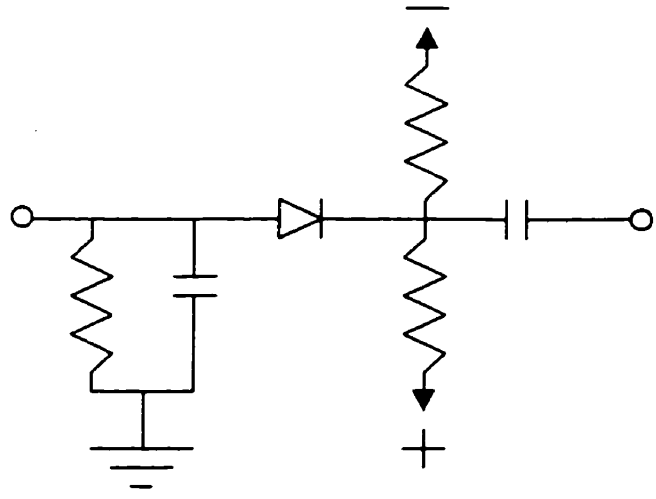

VARIABLE GAIN
AMPLIFIER

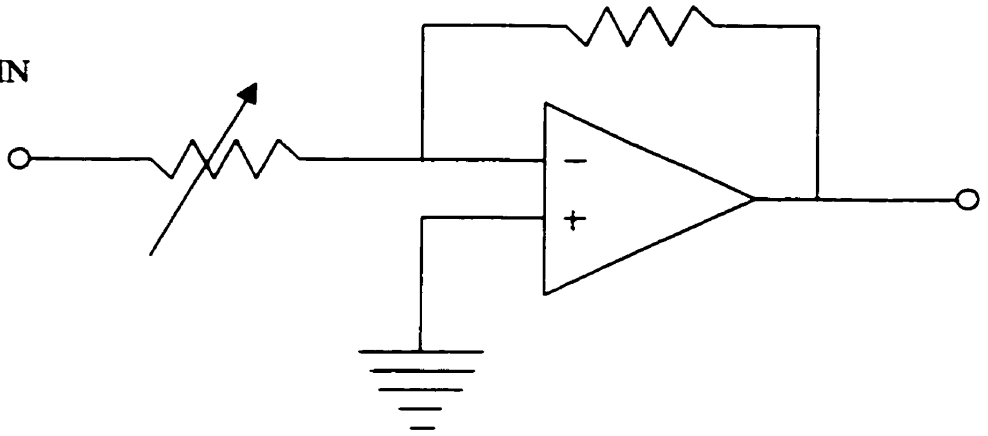

POWER SUPPLY
VOLTAGE SPLITTER

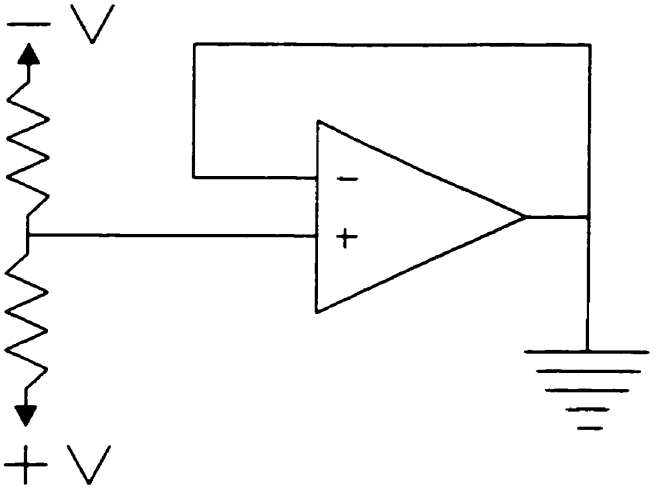

PHASE
SHIFTER